



3 4456 0550891 0

Cy 155

An Evaluation of the HSST Program Intermediate Pressure Vessel Tests in Terms of Light-Water-Reactor Pressure Vessel Safety

J. G. Merkle
G. D. Whitman
R. H. Bryan

OAK RIDGE NATIONAL LABORATORY
CENTRAL RESEARCH LIBRARY
DOCUMENT COLLECTION

LIBRARY LOAN COPY

DO NOT TRANSFER TO ANOTHER PERSON

If you wish someone else to see this
document, send in name with document
and the library will arrange a loan.

JUN 1964
15 3 67



OAK RIDGE NATIONAL LABORATORY

OPERATED BY UNION CARBIDE CORPORATION • FOR THE U.S. ATOMIC ENERGY COMMISSION

Printed in the United States of America. Available from
National Technical Information Service
U.S. Department of Commerce
5285 Port Royal Road, Springfield, Virginia 22161
Price: Printed Copy \$5.45; Microfiche \$2.25

This report was prepared as an account of work sponsored by the United States Government. Neither the United States nor the Energy Research and Development Administration, nor any of their employees, nor any of their contractors, subcontractors, or their employees, makes any warranty, express or implied, or assumes any legal liability or responsibility for the accuracy, completeness or usefulness of any information, apparatus, product or process disclosed, or represents that its use would not infringe privately owned rights.

Contract W-7405-eng-26

Reactor Division

AN EVALUATION OF THE HSST PROGRAM INTERMEDIATE
PRESSURE VESSEL TESTS IN TERMS OF LIGHT-
WATER-REACTOR PRESSURE VESSEL SAFETY

J. G. Merkle G. D. Whitman
R. H. Bryan

Work funded by the Nuclear Regulatory Commission
under Interagency Agreement 40-495-75

NOVEMBER 1975

NOTICE This document contains information of a preliminary nature
and was prepared primarily for internal use at the Oak Ridge National
Laboratory. It is subject to revision or correction and therefore does
not represent a final report.

OAK RIDGE NATIONAL LABORATORY
Oak Ridge, Tennessee 37830
operated by
UNION CARBIDE CORPORATION
for the
U.S. ENERGY RESEARCH AND DEVELOPMENT ADMINISTRATION



3 4456 0550891 0

CONTENTS

| | Page |
|---|------|
| FOREWORD | v |
| SUMMARY | ix |
| INTRODUCTION | 1 |
| VESSEL DESIGN AND FABRICATION | 5 |
| MATERIALS INVESTIGATIONS | 9 |
| TEST CONDITIONS | 10 |
| FLAW PREPARATION | 10 |
| MODEL TESTS | 11 |
| TESTS RESULTS AND ANALYSES | 11 |
| Tests with Transition Range Toughness | 17 |
| Tests with Static Upper-Shelf Toughness | 22 |
| Tests with Static and Dynamic Upper-Shelf Toughness | 24 |
| EXAMPLE CALCULATIONS FOR A HYPOTHETICAL REACTOR | |
| PRESSURE VESSEL | 32 |
| Definition of the Reference Computational Model | 32 |
| Fracture Toughness Estimates | 34 |
| Stress-Strain Properties and Pressure-Strain Calculations ... | 35 |
| Code Design Pressure | 38 |
| Upper-Shelf Plastic Instability Pressures | 38 |
| Linear Elastic Fracture Mechanics Calculations | 40 |
| Elastic-Plastic Fracture Mechanics Calculations | 42 |
| ASME Code, Section III, Appendix G Calculations | 44 |
| DISCUSSION | 45 |
| REFERENCES..... | 46 |

FOREWORD

The work reported herein was performed mostly at the Oak Ridge National Laboratory under the Heavy-Section Steel Technology (HSST) Program which is managed by G. D. Whitman. The HSST program is under the sponsorship of the U.S. Nuclear Regulatory Commission (NRC). The manager for the NRC is E. K. Lynn.

This report is designated Heavy-Section Steel Technology Program Technical Report No. 39. Prior reports in this series are:

1. S. Yukawa, *Evaluation of Periodic Proof Testing and Warm Prestressing Procedures for Nuclear Reactor Vessels*, HSSTP-TR-1, General Electric Company, Schenectady, N.Y. (July 1, 1969).
2. L. W. Loechel, *The Effect of Section Size on the Transition Temperature in Steel*, MCR-69-189, Martin Marietta Corporation, Denver, Colo. (Nov. 20, 1969).
3. P. N. Randall, *Gross Strain Measure of Fracture Toughness of Steels*, HSSTP-TR-3, TRW Systems Group, Redondo Beach, Calif. (Nov. 1, 1969).
4. C. Visser, S. E. Gabrielse, and W. VanBuren, *A Two-Dimensional Elastic-Plastic Analysis of Fracture Test Specimens*, WCAP-7368, Westinghouse Electric Corporation, PWR Systems Division, Pittsburgh, Pa. (October 1969).
5. T. R. Mager, F. O. Thomas, and W. S. Hazelton, *Evaluation by Linear Elastic Fracture Mechanics of Radiation Damage to Pressure Vessel Steels*, WCAP-7328, Revised, Westinghouse Electric Corporation, PWR Systems Division, Pittsburgh, Pa. (October 1969).
6. W. O. Shabbits, W. H. Pryle, and E. T. Wessel, *Heavy Section Fracture Toughness Properties of A533 Grade B Class 1 Steel Plate and Submerged Arc Weldment*, WCAP-7414, Westinghouse Electric Corporation, PWR Systems Division, Pittsburgh, Pa. (December 1969).
7. F. J. Loss, *Dynamic Tear Test Investigations of the Fracture Toughness of Thick-Section Steel*, NRL-7056, U. S. Naval Research Laboratory, Washington, D.C. (May 14, 1970).
8. P. B. Crosley and E. J. Ripling, *Crack Arrest Fracture Toughness of A533 Grade B Class 1 Pressure Vessel Steel*, HSSTP-TR-8, Materials Research Laboratory, Inc., Glenwood, Ill. (March 1970).
9. T. R. Mager, *Post-Irradiation Testing of 2T Compact Tension Specimens*, WCAP-7561, Westinghouse Electric Corporation, PWR Systems Division, Pittsburgh, Pa. (August 1970).

10. T. R. Mager, *Fracture Toughness Characterization Study of A533, Grade B, Class 1 Steel*, WCAP-7578, Westinghouse Electric Corporation, PWR Systems Division, Pittsburgh, Pa. (October 1970).
11. T. R. Mager, *Notch Preparation in Compact Tension Specimens*, WCAP-7579, Westinghouse Electric Corporation, PWR Systems Division, Pittsburgh, Pa. (November 1970).
12. N. Levy and P. V. Marcal, *Three-Dimensional Elastic-Plastic Stress and Strain Analysis for Fracture Mechanics, Phase I: Simple Flawed Specimens*, HSSTP-TR-12, Brown University, Providence, R.I. (December 1970).
13. W. O. Shabbits, *Dynamic Fracture Toughness Properties of Heavy Section A533 Grade B, Class 1 Steel Plate*, WCAP-7623, Westinghouse Electric Corporation, PWR Systems Division, Pittsburgh, Pa. (December 1970).
14. P. N. Randall, *Gross Strain Crack Tolerance of A533-B Steel*, HSSTP-TR-14, TRW Systems Group, Redondo Beach, Calif. (May 1, 1971).
15. H. T. Corten and R. H. Sailors, *Relationship Between Material Fracture Toughness Using Fracture Mechanics and Transition Temperature Tests*, T&AM Report No. 346, University of Illinois, Urbana, Ill. (August 1, 1971).
16. T. R. Mager and V. J. McLoughlin, *The Effect of an Environment of High Temperature Primary Grade Nuclear Reactor Water on the Fatigue Crack Growth Characteristics of A533 Grade B Class 1 Plate and Weldment Material*, WCAP-7776, Westinghouse Electric Corporation, PWR Systems Division, Pittsburgh, Pa. (October 1971).
17. N. Levy and P. V. Marcal, *Three-Dimensional Elastic-Plastic Stress and Strain Analysis for Fracture Mechanics, Phase II: Improved Modeling*, HSSTP-TR-17, Brown University, Providence, R.I. (November 1971).
18. S. C. Grigory, *Six-Inch-Thick Flawed Tensile Tests, First Technical Summary Report, Longitudinal Specimens 1 through 7*, HSSTP-TR-18, Southwest Research Institute, San Antonio, Tex. (June 1972).
19. P. N. Randall, *Effects of Strain Gradients on the Gross Strain Crack Tolerance of A533-B Steel*, HSSTP-TR-19, TRW Systems Group, Redondo Beach, Calif. (May 1, 1972).
20. S. C. Grigory, *Tests of Six-Inch-Thick Flawed Tensile Specimens, Second Technical Summary Report, Transverse Specimens Numbers 8 through 10, Welded Specimens Numbers 11 through 13*, HSSTP-TR-20, Southwest Research Institute, San Antonio, Tex. (June 1972).

21. L. A. James and J. A. Williams, *Heavy Section Steel Technology Program Technical Report No. 21, The Effect of Temperature and Neutron Irradiation upon the Fatigue-Crack Propagation Behavior of ASTM A533, Grade B, Class 1 Steel*, HEDL-TME 72-132, Hanford Engineering Development Laboratory, Richland, Wash. (September 1972).
22. S. C. Grigory, *Tests of Six-Inch-Thick Flawed Tensile Specimens, Third Technical Summary Report, Longitudinal Specimens Numbers 14 through 16, Unflawed Specimen Number 17*, HSSTP-TR-22, Southwest Research Institute, San Antonio, Tex. (October 1972).
23. S. C. Grigory, *Tests of Six-Inch-Thick Flawed Tensile Specimens, Fourth Technical Summary Report, Tests of One-Inch-Thick Flawed Tensile Specimens for Size Effect Evaluation*, HSSTP-TR-23, Southwest Research Institute, San Antonio, Tex. (June 1973).
24. S. P. Ying and S. C. Grigory, *Tests of Six-Inch-Thick Tensile Specimens, Fifth Technical Summary Report, Acoustic Emission Monitoring of One-Inch and Six-Inch-Thick Tensile Specimens*, HSSTP-TR-24, Southwest Research Institute, San Antonio, Tex. (November 1972).
25. R. W. Derby et al., *Test of 6-Inch-Thick Pressure Vessels, Series 1: Intermediate Test Vessels V-1 and V-2*, ORNL-4895, Oak Ridge National Laboratory, Oak Ridge, Tenn. (February 1974).
26. W. J. Stelzman and R. G. Berggren, *Radiation Strengthening and Embrittlement in Heavy Section Plates and Welds*, ORNL-4871, Oak Ridge National Laboratory, Oak Ridge, Tenn. (June 1973).
27. P. B. Crosley and E. J. Ripling, *Crack Arrest in an Increasing K-Field*, HSSTP-TR-27, Materials Research Laboratory, Glenwood, Ill. (January 1973).
28. P. V. Marcal, P. M. Stuart, and R. S. Bettles, *Elastic-Plastic Behavior of a Longitudinal Semi-Elliptical Crack in a Thick Pressure Vessel*, HSSTP-TR-28, Brown University, Providence, R.I. (June 1973).
29. W. J. Stelzman, *Characterization of HSST Plate 02* (in preparation).
30. D. A. Canonico, *Characterization of Heavy Section Weldments in Pressure Vessel Steels* (in preparation).
31. J. A. Williams, *The Irradiation and Temperature Dependence of Tensile and Fracture Properties of ASTM A533, Grade B, Class 1 Steel Plate and Weldment*, HEDL-TME 73-75, Hanford Engineering Development Laboratory, Richland, Wash. (August 1973).
32. J. M. Steichen and J. A. Williams, *High Strain Rate Tensile Properties of Irradiated ASTM A533 Grade B Class 1 Pressure Vessel Steel*, HEDL-TME 73-74, Hanford Engineering Development Laboratory, Richland, Wash. (July 1973).

33. P. C. Riccardella and J. L. Swedlow, *A Combined Analytical-Experimental Fracture Study*, WCAP-8224, Westinghouse Electric Corporation, PWR Systems Division, Pittsburgh, Pa. (October 1973).
34. R. J. Podlasek and R. J. Eiber, *Final Report on Investigation of Mode III Crack Extension in Reactor Piping*, HSSTP-TR-34, Battelle Columbus Laboratories, Columbus, Ohio (May 1974).
35. T. R. Mager et al., *Interim Report on the Effect of Low Frequencies on the Fatigue Crack Growth Characteristics of A533 Grade B Class 1 Plate in an Environment of High-Temperature Primary Grade Nuclear Reactor Water*, WCAP-8256, Westinghouse Electric Corporation, Pittsburgh, Pa. (December 1973).
36. J. A. Williams, *The Irradiated Fracture Toughness of ASTM A533, Grade B, Class 1 Steel Measured with a Four Inch Thick Compact Tension Specimen*, HEDL-TME 75-10, Hanford Engineering Development Laboratory, Richland, Wash. (January 1975).
37. R. H. Bryan et al., *Test of 6-Inch-Thick Pressure Vessels, Series 2. Intermediate Test Vessels V-3, V-4 and V-6*, ORNL-5059, Oak Ridge National Laboratory, Oak Ridge, Tenn. (to be published).
38. T. R. Mager, S. E. Yanichko, and L. R. Singer, *Fracture Toughness Characterization of HSST Intermediate Pressure Vessel Material*, WCAP-8456, Westinghouse Electric Corporation, Pittsburgh, Pa. (December 1974).

SUMMARY

The Heavy-Section Steel Technology (HSST) Program is sponsored by the Reactor Safety Research Division of the Nuclear Regulatory Commission. Under the program, eight 6-in.-thick 39-in.-OD steel pressure vessels containing carefully prepared and sharpened surface cracks have been tested to provide an improved quantitative basis for evaluating the safety margins against fracture of nuclear reactor pressure vessels. The test results furnish direct evidence of the high fracture resistance of the steels used for fabricating light-water reactor pressure vessels and provide a vital basis for developing and verifying the analytical methods required for calculating safety margins against fracture.

The cylindrical regions of the test vessels were fabricated from either A508 class 2 forging steel or A533, grade B, class 1 steel plate. Ten vessels were fabricated, two of which remain to be tested, one containing an A508 forged nozzle and the other having a plain cylindrical region of A533, grade B, class 1 steel. Of the eight vessels tested, two contained external surface cracks in A508 class 2 forging steel, three contained at least one external surface crack in weld metal, two contained inside nozzle corner cracks in A508 forged nozzles, and one contained a very deep external surface crack in A533, grade B, class 1 steel. All the eight vessels tested were loaded to failure by internal hydraulic pressure.

Flaws in the test vessels ranged from 1.20 to 5.30 in. in depth, and test temperatures ranged from 32 to 196°F. Extensive fast fracture was observed, as expected, at 32°F at a pressure near the gross yield pressure of the test vessel, and two vessels leaked without fracturing at or slightly above 190°F. One of these vessels contained a flawed nozzle, and the other contained a very deep external surface flaw. Another vessel containing a smaller external surface flaw achieved 2% strain in the plastic range at 190°F before developing a shear fracture that arrested before reaching the ends of the vessel.

Extensive pre- and posttest fracture analyses have been performed for all the intermediate vessels tested. An important element in these analyses was the use of fracture toughness values obtained from small-specimen

test data by methods of elastic-plastic fracture analysis developed for this purpose by the HSST program. In addition, numerous fracture experiments have been performed with sharp flawed steel and epoxy models. These models have provided extremely valuable strain analysis and fracture data, as well as reliable linear elastic fracture mechanics calibrations for cracks in nozzle corner regions, which are still difficult to obtain analytically. An effort to develop an accurate three-dimensional, elastic-plastic, finite-element analysis of a flawed nozzle corner region is continuing in preparation for the testing of the remaining intermediate test vessel containing a nozzle.

The analytical studies performed indicate that below the upper-shelf temperature range, linear elastic fracture mechanics (expressed in terms of strain) is accurate or conservative, depending on transverse restraint conditions prior to the onset of through-thickness yielding. In addition, in the cylindrical region of a vessel, within the upper-shelf temperature range, failure is controlled by the onset of plastic instability in the region surrounding the flaw if the upper-shelf toughness is sufficiently high. For surface flaws less than half the test vessel wall thickness in depth, failure loads were approximately three times the code design pressure of the test vessels.

Application of the analysis procedures developed for the intermediate test vessels to a hypothetical reactor pressure vessel indicates that a similar margin of safety is inherent in full-scale vessels. Although linear elastic fracture mechanics expressed in terms of strain is applicable to full-scale vessels prior to the onset of through-thickness yielding, it is too conservative above the gross yield pressure for realistically estimating the upper-shelf toughness required to reach plastic instability conditions. Elastic-plastic fracture analysis methods are required for this purpose, and calculations by one such method are included in the example analysis of the hypothetical full-scale vessel. The conservatism of the present ASME code procedures for fracture safety analyses that are based on the K_{IR} curve is also illustrated by the example calculations.

AN EVALUATION OF THE HSST PROGRAM INTERMEDIATE PRESSURE VESSEL
TESTS IN TERMS OF LIGHT-WATER-REACTOR PRESSURE VESSEL SAFETY

J. G. Merkle G. D. Whitman
R. H. Bryan

INTRODUCTION

Testing of the intermediate pressure vessels is a major activity under the Heavy-Section Steel Technology Program. A primary objective of these tests is to develop or verify methods of fracture prediction through the testing of selected structures and materials so that a valid basis can be established for evaluating the serviceability and safety of light-water reactor (LWR) pressure vessels. This is a preliminary report of the results of the tests already conducted and of some of the implications of the results with respect to the safety against fracture of reactor pressure vessels.

The intermediate pressure vessel tests and the methods of fracture prediction applied to them are an important part of the total effort that is made to achieve the high quality of reactor pressure vessels required for the protection of the public health and safety.

Structural integrity of reactor pressure vessels is established by designing and fabricating them in accordance with the applicable ASME code and Nuclear Regulatory Commission (NRC) requirements for nuclear pressure vessels, by inspecting for flaws of significant size, and by evaluating the safety margin available against fracture should flaws exist or develop during operation. The event that must be avoided in service is a fracture, without prior warning, in a reactor pressure vessel that can disrupt the safety features of the nuclear reactor plant. Reactor pressure vessels were known to possess a large margin of safety against failure under anticipated operating conditions, but the influence of flaws on this margin had not been quantitatively determined for many situations of interest before the start of the HSST program. A dependable evaluation of safety margin can only be accomplished with verified analytical methods involving the utilization of a detailed stress analysis, pertinent material properties, and a geometrical description of the hypothetical or real flaw.

The intermediate vessel tests were planned with sufficiently specific objectives that substantial quantitative weight could be given to the results. Each set of testing conditions was chosen so as to provide specific quantitative data by which analytical methods of predicting flaw growth, and in some cases crack arrest, could be evaluated. Every practical effort was made to assure that results would be relevant to some aspect of real reactor pressure vessel performance through careful control of material properties, selection of test temperatures, and design of prepared flaws.

The intermediate test vessels were fabricated from the same low-alloy steels used in the fabrication of LWR pressure vessels, typical examples of which are shown in Figs. 1 and 2. Sharp flaws of desired size, location, and orientation were produced in each test vessel; and they were then loaded by internal pressure so that the state of stress achieved in deliberately flawed regions was similar to the state of stress that would exist in a full-scale reactor vessel if it were to contain a flaw. The intermediate test vessels are smaller in diameter and wall thickness than actual reactor pressure vessels, but the thickness chosen and the internal pressures used in the tests are adequate for providing the relevant conditions in the neighborhood of the prepared flaw. Each test was continued until failure occurred, in every case at a loading substantially in excess of the design load. The use of pressures and, in some tests, temperatures more severe than occur during any condition specified for real reactor pressure vessels was necessary in order to obtain quantitative data by which methods of fracture prediction could be evaluated.

The tests, in addition to providing experimental data on fracture strength to verify analytical methods, directly demonstrated the behavior of thick-section vessels with flaws present. The major emphasis in these tests was placed on measuring the conditions (stress and strain) at the onset of flaw instability. Analytical methods that relate these conditions to material properties, temperature, internal pressure, and flaw configuration are required for the determination of the factor of safety against disruptive failure.

In addition to the information of primary interest, data were also obtained on crack propagation, crack arrest, and failure mode; and in

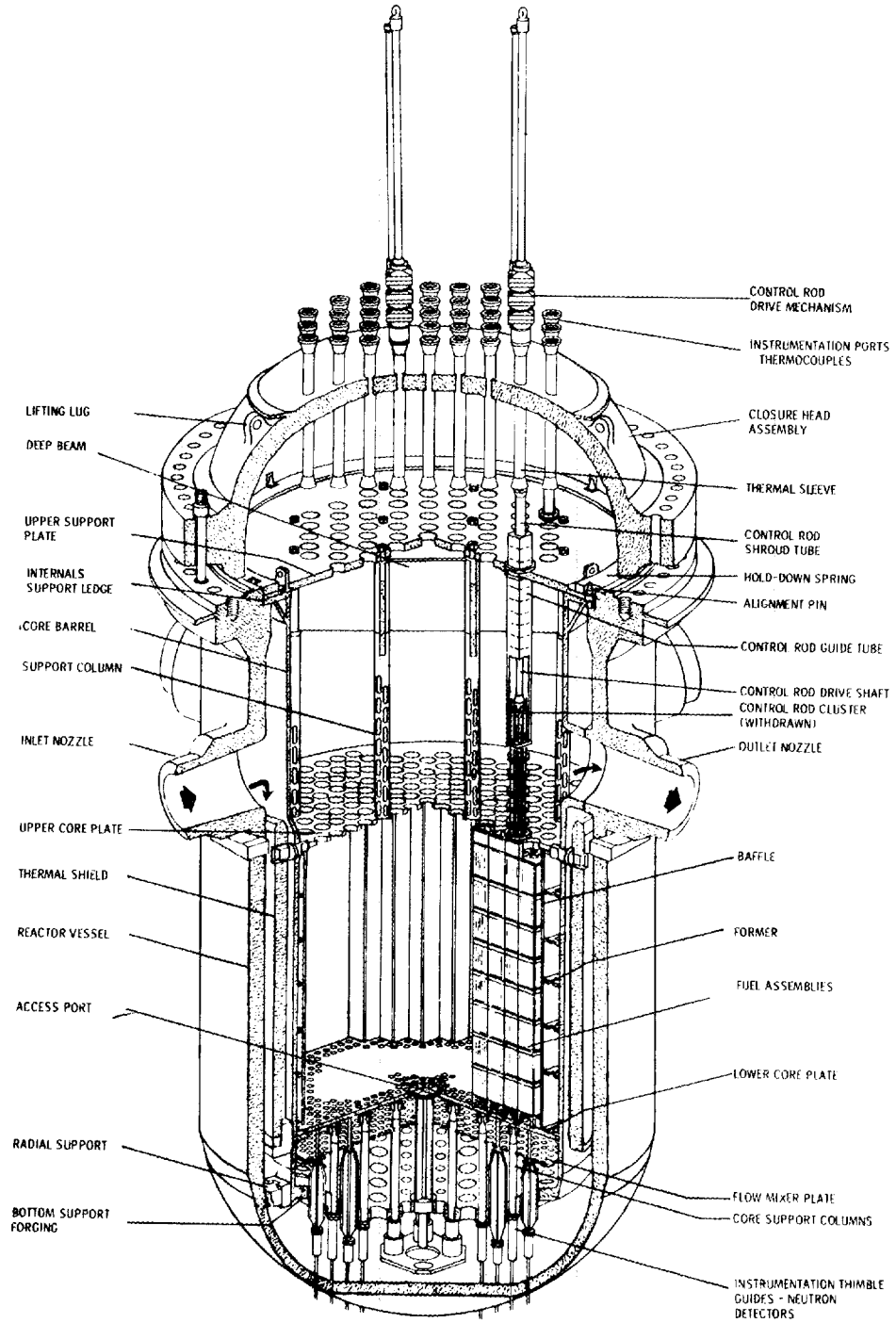


Fig. 1. Typical PWR pressure vessel and internals.

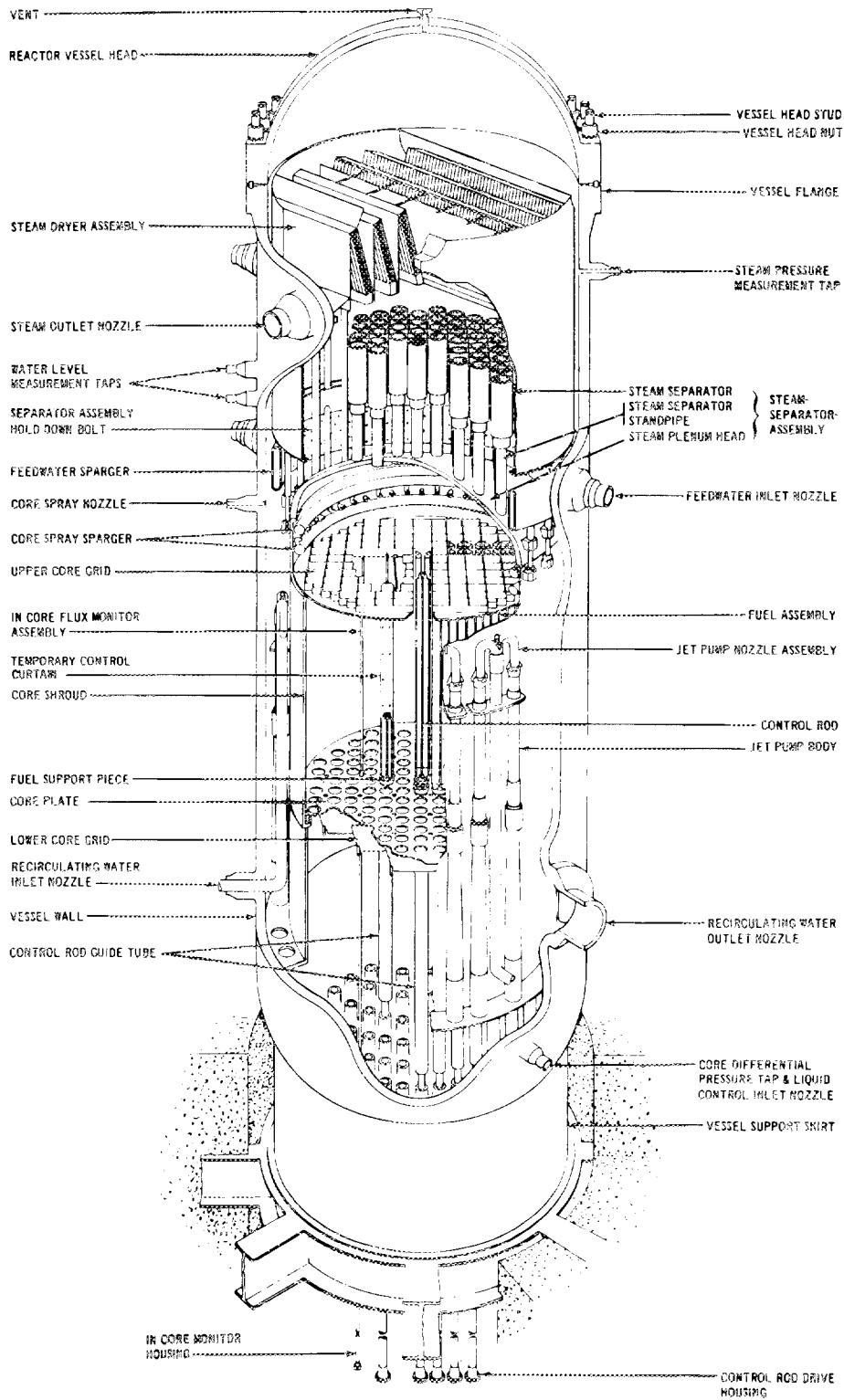


Fig. 2. Typical BWR pressure vessel and internals.

certain instances only stable crack growth leading to "leak before break" was observed under the conditions of a particular test. Although these secondary observations are pertinent to the behavior of the steels used in LWR vessels, the tests were not designed to provide conclusive data for the verification of analytical methods concerned with the terminal behavior of propagating cracks. Predictions of the ultimate failure modes of reactor vessels must be made with due consideration given to the greater amount of energy contained in the pressurized-water reactor (PWR) or the boiling-water reactor (BWR) systems. Nevertheless, the intermediate vessel tests have provided direct evidence as to either the very large flaws or the severe deterioration of materials properties that would have to develop in a reactor pressure vessel before an abrupt and disruptive failure could occur.

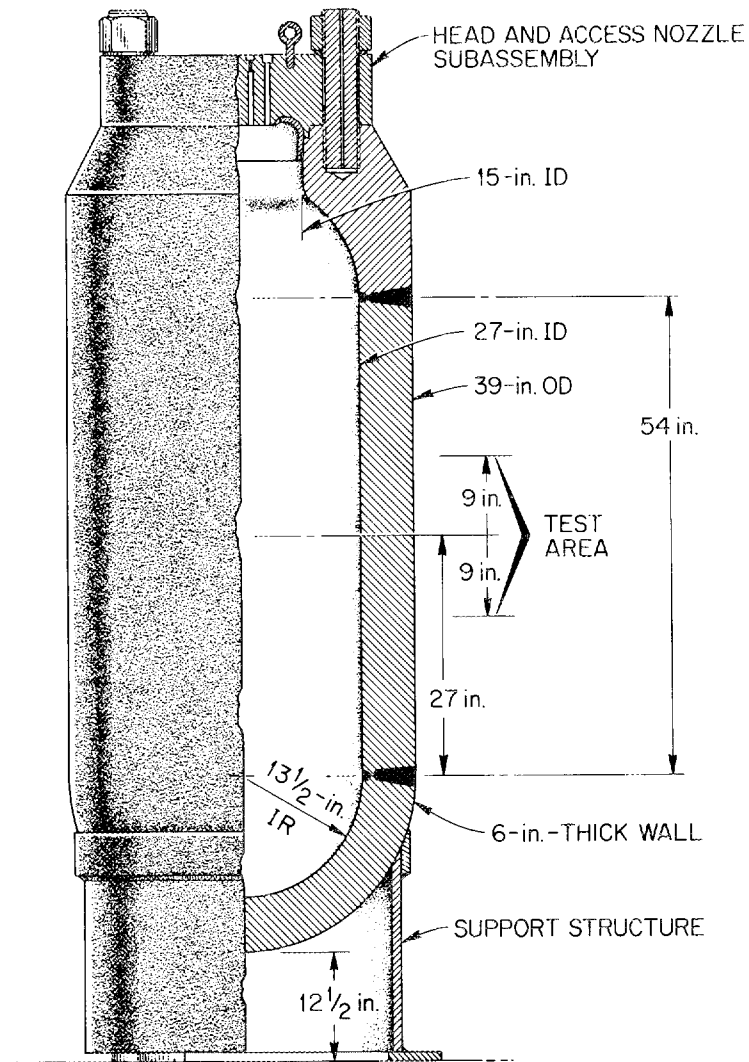
VESSEL DESIGN AND FABRICATION

The design and fabrication of the intermediate vessels have been previously described,¹ and only a brief review of this aspect of the project will be covered here.

There are ten vessels in the test series. Figure 3 shows a partially sectioned view of vessels V-1, V-2, V-3, V-4, V-6, V-7, and V-8; Fig. 4 shows a sectioned view of vessels V-5, V-9, and V-10. The materials of construction are listed in Table 1, and the orientation of the welds in the cylindrical test sections of vessels V-3, V-4, and V-6 through V-10 are shown in Fig. 5.

The vessels were designed and fabricated in accordance with the 1968 edition of Section III of the ASME Boiler and Pressure Vessel Code. In addition to the normal quality assurance provisions of the code, an additional inspection requirement was imposed for all the welds, namely that both longitudinal and shear beam ultrasonic testing be performed.

The vessels were sized to permit entry of a man into the vessel, and the length of the cylindrical section was determined by specifying that the stress in the test section of the cylinder should be unaffected by the head regions. The wall thickness was chosen so that a valid test of the theory and methods of linear elastic fracture mechanics would be



Intermediate Test Vessels.

Fig. 3. HSST intermediate vessel.

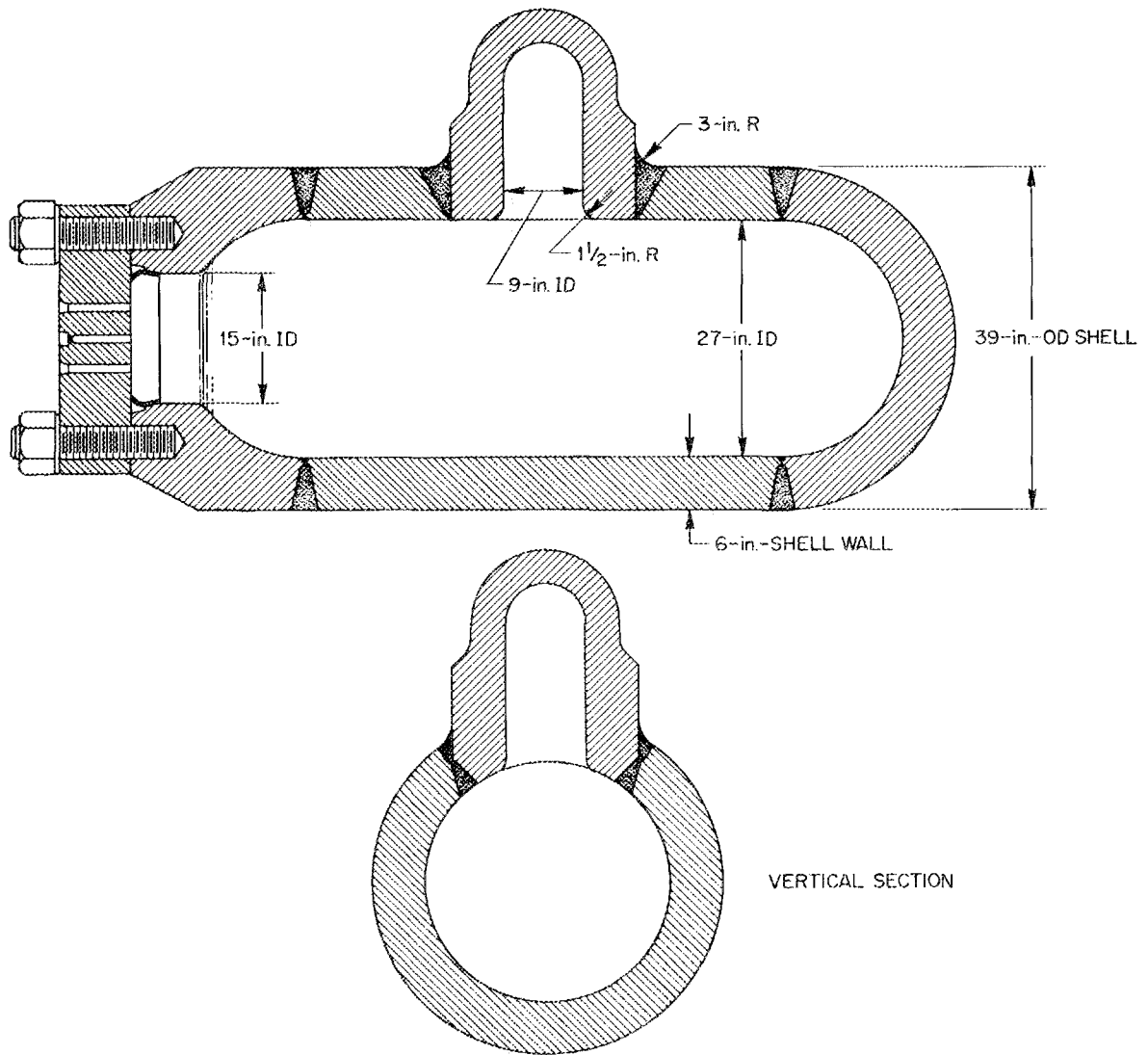


Fig. 4. HSST intermediate vessel with 9-in.-ID test nozzle.

within the capabilities of the test facility. Specifically, a 6-in. wall is thick enough for such a test at temperatures attainable in the facility and with prepared surface flaws extending less than halfway through the wall. A typical PWR pressure vessel (Fig. 1) has a design pressure rating of 2500 psi, and a typical BWR pressure vessel (Fig. 2) has a design pressure rating of 1250 psi; the intermediate vessel cylinders have a design pressure of 9710 psi because of their smaller diameter-to-thickness ratio

Table 1. Materials used for fabricating intermediate test vessel cylinders and nozzles

| Vessel designation | Material | |
|--------------------|-------------------|--------------|
| | Cylindrical shell | Nozzle |
| V-1 | A508 class 2 | |
| V-2 | A508 class 2 | |
| V-3 | A508 class 2 | |
| V-4 | A508 class 2 | |
| V-5 | A508 class 2 | A508 class 2 |
| V-6 | A508 class 2 | |
| V-7 | A533-B class 1 | |
| V-8 | A533-B class 1 | |
| V-9 | A533-B class 1 | A508 class 2 |
| V-10 | A533-B class 1 | A508 class 2 |

ORNL-DWG 73-5413

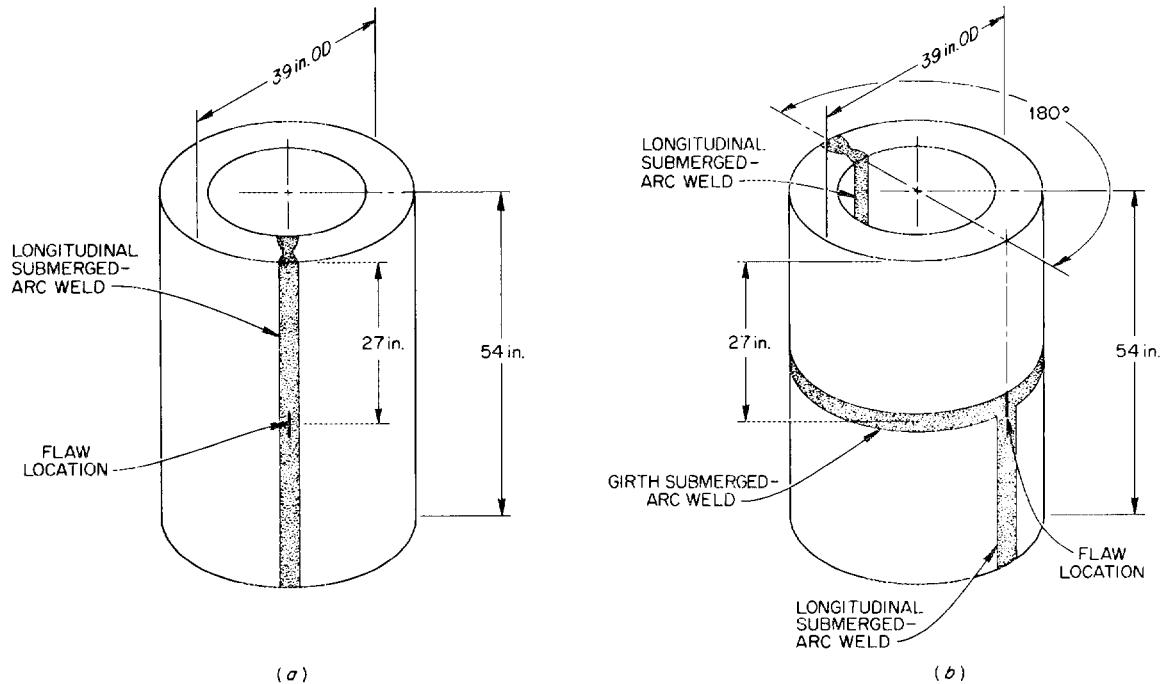


Fig. 5. Weld orientation for (a) vessels 3, 4, 7, 8, 9, 10; (b) vessel 6.

compared to actual LWR vessels. By definition, the difference between the largest and the smallest principal stresses at design pressure is the same in the test vessels as in the real reactor vessels.

The radially attached nozzle shown in Fig. 4 that was designed into three of the vessels (V-5, V-9, and V-10) was proportioned to give a representative state of stress for nozzles permitted by the ASME code. Both finite-element and experimental strain analyses were performed on this structure to verify the design.

Some difficulty was encountered in controlling the material properties for the first six vessels, which contained cylindrical regions of A508 class 2 forging steel. The chemistry of this steel was such that untypically high strength and toughness properties were originally achieved, and retempering at 1320°F was required to achieve typical properties.

MATERIALS INVESTIGATIONS

Extensive characterization of the materials in the cylindrical sections was achieved with mechanical property and fracture toughness specimens taken from 2-ft-long prolongations of the vessel cylinders made by the same fabrication procedures as the cylinders themselves. Tensile, Charpy V-notch impact energy, and drop-weight nil ductility transition temperature tests were conducted on prolongation material using location (depth from surface) as a variable. Compact-tension (fracture mechanics) specimens varying from 0.394 to 4 in. thick were also tested. In addition, 1/7-scale model vessels fabricated from the prolongation material were tested prior to testing the corresponding intermediate-size prototype.

The intermediate vessel tests were preceded by a considerable development effort related to the use of small specimens for determining fracture toughness properties over a wide range of temperatures.²⁻⁴ Material fracture toughness properties obtained from specimens as small as Charpy-size specimens provided data that were successfully used in predicting fracture behavior. The establishment of methods permitting the use of small specimens to determine fracture toughness greatly enhances the value of the surveillance specimens used in LWRs.

TEST CONDITIONS

Tests were performed over a temperature range sufficiently broad to cover frangible, transitional, and ductile fracture behavior. Frangible failure occurs at low temperatures without warning, and there is little or no nominal plastic strain associated with the failure. This mode of failure occurs at stress levels equal to or less than the yield stress, and crack propagation is rapid and extensive. Transitional failure occurs at intermediate temperatures between the limits of totally frangible and totally ductile behavior. Interest in this region stems primarily from the need to know the limits of applicability of linear elastic fracture mechanics (LEFM) analysis in the transition range of temperature. Ductile behavior occurs at higher temperatures and requires energy input from the applied load for continued crack extension, and crack propagation velocity is reduced relative to frangible behavior. Ductile failure may occur because of very large flaws or overload. In keeping with the purpose of establishing a basis for quantitatively assessing safety margins, the tests were always carried to overload, in comparison with normal or expected reactor pressure vessel conditions.

FLAW PREPARATION

An important factor in the testing of the intermediate vessels was the provision for properly shaped and sharpened flaws. For investigating frangible behavior, this provision is necessary to meet the conditions of crack sharpness required to ensure the applicability of LEFM. In the transitional and tough regimes of failure, crack sharpness may affect the extent of stable crack growth prior to reaching maximum load. Therefore, it is important to obtain crack sharpness typical of naturally occurring fatigue cracks for these regimes also. All the intermediate vessel tests have been performed with sharpened flaws so as to simulate the characteristics of the most serious defects that could occur in pressure vessels.

Except for vessel V-7, the machined notches in the test vessels were sharpened by pressure pulsing the void formed by machining. The large flaw in intermediate test vessel V-7 was sharpened by hydrogen charging an electron-beam weld zone at the root of the machined notch. The flaws

in the model vessels were also sharpened by electron-beam welding and hydrogen charging.

Pulse-echo, shear wave, and dynamic base-line noise-monitoring ultrasonic techniques were used to monitor crack growth. In some instances, correlations between crack growth and crack-opening-displacement measurements were also made.

MODEL TESTS

Scale-model tests have been used extensively as an aid to the planning and the interpretation of the results of the intermediate pressure vessel tests. The models were of two types: epoxy models, such as those shown in Fig. 6, the behavior of which was elastic; and steel models, such as those shown in Fig. 7, the behavior of which was elastic-plastic. Both types of models contained machined notches that were converted to sharp cracks by sharpening the notch tips -- in the case of the epoxy model vessels by fatigue and in the case of the steel models by electron-beam welding followed by hydrogen charge cracking. Both types of models provided experimental strain analysis data that accurately depicted the behavior of their respective intermediate size prototypes prior to failure. In addition, selected data were used as input to some of the analytical predictions of the fracture strength of the intermediate test vessels. The experimental strain data from models were especially valuable for characterizing the nozzle-to-cylinder junction region, for which three-dimensional finite-element predictions did not agree with experimental data. The model fracture data provided an indispensable means for evaluating proposed fracture analysis methods in advance of their application to the intermediate test vessels. The model data are particularly useful for evaluating the ability of proposed analytical methods to properly consider flaw size and thickness effects over a sufficiently broad range of size.

TEST RESULTS AND ANALYSES

The plan for the intermediate vessel tests was to first conduct tests that could possibly have results that would preempt further tests or would

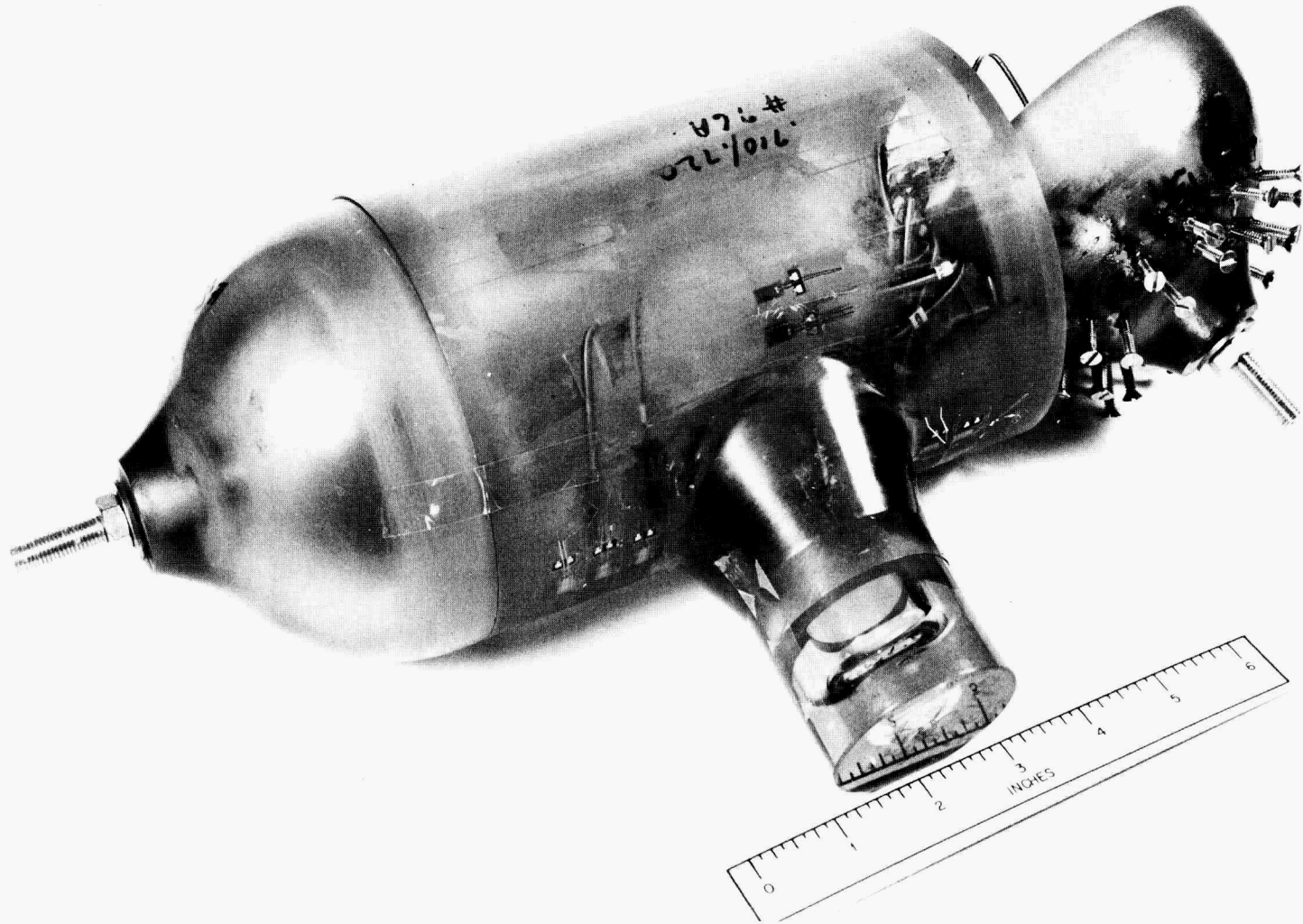


Fig. 6. Epoxy model vessel with nozzle.

PHOTO 1218-73



Fig. 7. One-seventh-scale steel models of intermediate test vessels.

necessitate a radical change in plans. Otherwise, the testing sequence was principally dependent upon the operational factors of conducting a first-of-its-kind experimental program. Thus, vessels V-1 through V-6 were procured first and were tested while vessels V-7 through V-10 were being designed, fabricated, and prepared for testing.

The testing conditions for the intermediate pressure vessel tests are given in Table 2, and the results obtained thus far are listed in Table 3. The vessels are listed in order of increasing test temperature, because of the controlling influence of temperature on the fracture toughness of the vessel material. The vessels were tested in ascending numerical order, except for the reversal in order of vessels V-5 and V-6.

The conditions for the first test (vessel V-1) were selected for a combination of reasons, some of which were concerned with demonstrating that the flaw preparation techniques and experimental methods developed with scale-model vessels and large-scale mockups would be satisfactory in testing the real vessels. The more fundamental reason for adopting the conditions of this test was the desire to test the hypothesis that crack initiation in material exhibiting high static upper-shelf toughness would not precede the onset of gross yielding. If this had not proven to be the case, subsequent tests would probably have been planned differently. As it turned out, predictions were satisfactorily confirmed in each successive test, so that the series of eight intermediate vessel tests were able to cover the three important ranges of fracture behavior as well as a range of flaw sizes and stress concentrations.

It can be seen from Tables 2 and 3 that, in addition to temperature, two other factors also have a strong influence on the conditions at failure, namely, flaw size and stress concentrations. As indicated by the results for vessels V-6 and V-7, vessel strength decreases as flaw size increases; and, as indicated by the results for vessels V-5 and V-9, if the flaw is located in a region of stress concentration the strength is reduced more.

Another factor that has a significant influence on the mode and extent of crack propagation is the difference between the resistance of the material to the onset of rapid fracture and the resistance of the material to the continued extension of a running crack. The former property of the

Table 2. Intermediate vessel test conditions

| Vessel No. | Flaw size (in.) | | Test temperature (°F) | Fracture toughness K_{Ic} (ksi $\sqrt{\text{in.}}$) | Flaw description | |
|------------|-----------------|--------|-----------------------|--|------------------|-----------------|
| | a | 2b | | | Location | Material |
| 2 | 2.53 | 8.30 | 32 | 184 | Outside | A508-2 |
| 4 | 3.00 | 8.25 | 75 | 160 | Outside | Weld |
| 9 | 1.20 | Nozzle | 75 | 150-275 | Inside | A508-2 (nozzle) |
| 1 | 2.56 | 8.25 | 130 | 311 | Outside | A508-2 |
| 3 | 2.11 | 8.50 | 130 | 325 | Outside | Weld |
| 6 | 1.87 | 5.25 | 190 | 369 | Outside | Weld |
| 5 | 1.20 | Nozzle | 190 | 241 | Inside | A508-2 (nozzle) |
| 7 | 5.30 | 18.6 | 196 | 301 | Outside | A533-B |

Table 3. Intermediate vessel test results

| Vessel No. | Maximum pressure | | Mode of failure | Calculated results | | Load factor $(p_f/p_d)^b$ | Remarks |
|------------|---|---------------------------|-----------------|---------------------------------------|---------------------|---------------------------|--------------------------------|
| | p_f (ksi) and strain λ_f (%) at failure | | | LEFM based on strain ^a | Plastic instability | | |
| 2 | p_f λ_f | 27.9 0.194 | Flat | 27.4 0.206 | | 2.87 | |
| 4 | p_f λ_f | 26.5 0.168 | Mixed | 26.2 0.163 | | 2.73 | Transition range |
| 9 | p_f λ_f | 26.9 1.05 ^c | Mixed | 13.5-18.4 0.070-0.096 ^c | | 2.77 | |
| 1 | p_f λ_f | 28.8 0.92 | Mixed | 27.5 0.345 | 29.9 ^d | 2.96 | Static upper shelf |
| 3 | p_f λ_f | 31.0 1.47 | Mixed | 27.5 0.398 | 31.5 ^d | 3.19 | Static upper shelf |
| 6 | p_f λ_f | 31.9 2.0 | Shear | 27.5 0.479 | 33.7 ^d | 3.28 | Static and dynamic upper shelf |
| 5 | p_f λ_f | 26.6 0.25 ^c | Leak | 19.1 0.100 | | 2.74 | Static and dynamic upper shelf |
| 7 | p_f λ_f | 21.4 0.12 | Leak | 20.8 0.109 | 19.1 | 2.20 | Static and dynamic upper shelf |

^aLinear elastic fracture mechanics.

^b p_d , design pressure = 9.71 ksi.

^cOutside circumferential strain 180° from nozzle.

^dAssuming 15% stable crack growth as suggested in Ref. 1.

material is greater than the latter at temperatures below the normal range of operating temperature of reactor pressure vessels, but the reverse may even be true in the operating temperature range. At the present time, for analytical purposes, we are accepting the assumption that the same method of analysis is capable of describing both phenomena, providing that the correct numerical value of the fracture toughness is used for each case. Having to make this assumption leaves the scientific basis of experimental results open to further examination; but as an approximation the hypothesis has enough experimental justification to warrant its use in evaluating the conditions governing potential crack propagation in reactor pressure vessels.

Fracture analysis is an area of solid mechanics that is still under development. It is generally agreed that the methods of linear elastic fracture mechanics (LEFM) do describe the behavior of specimens that are completely brittle and fail without yielding. However, nuclear pressure vessels, like most engineering structures, are designed and built of materials that are capable of yielding extensively before failing. Although the LEFM method can be used to ensure that a specified flaw will not cause fracture before yielding, it may considerably underestimate the actual failure strain if gross yielding precedes fracture. Elastic-plastic methods of fracture analysis are more appropriate for these latter conditions. The model and intermediate pressure vessel test data obtained by the HSST program have provided valuable information regarding the fracture performance of pressure vessels in the inelastic range. These data have already been used as a basis for developing and testing methods of elastic-plastic fracture analysis,^{1,5} and they will continue to serve this important function in the future. An example application of elastic and elastic-plastic fracture analysis methods to a hypothetical reactor pressure vessel appears in a later section of this report.

Tests with Transition Range Toughness

The test that provided the best direct demonstration of the capabilities of LEFM was the test of vessel V-2. The test temperature for this vessel was 32°F, which is only 22°F above the estimated nil ductility

transition (NDT) temperature of the vessel material. This test temperature represents a much closer approach to the NDT temperature than would be permitted for an actual reactor pressure vessel under full load in service. Although brittle behavior was expected, some yielding was also expected prior to the onset of rapid fracture, and the effect of this yielding on the accuracy of a prediction based on LEFM was not known in advance. The test results indicated that the fracture strain for a flaw in the cylindrical region of the vessel could be accurately predicted by LEFM, provided that yielding had not progressed completely through the vessel wall. It appears that this is true because effectively no plastic strain occurs in the axial direction, tangential to the crack tip, and therefore a condition of full transverse restraint is maintained along the crack front even after partial yielding has occurred. When applying LEFM based on strain, as in the case of vessel V-2, the failure strain is calculated directly as if it were a totally elastic strain, and the corresponding pressure is then determined from the nonlinear pressure strain curve for the flaw location, ignoring the presence of the flaw. A calculated pressure vs outside surface circumferential strain curve for an intermediate test vessel is shown in Fig. 8. Because of the low test temperature, crack propagation in vessel V-2 was extensive, as shown in Fig. 9, including the separation of a piece of the vessel wall from the remainder of the vessel.

The test temperature for vessel V-4 was 75°F, but both the failure pressure and strain were slightly less than for vessel V-2. Vessel V-4 contained two flaws; the one at which failure initiated was located in a longitudinal weld that exhibited considerable variability in its fracture toughness properties. Posttest analysis indicated that the fracture toughness of the V-4 weld zone material that contained the critical flaw was 20% less than had been estimated before the test. Furthermore, this value was less than the fracture toughness of the material in vessel V-2. With this adjustment, the failure conditions for both vessels V-2 and V-4 are calculated quite closely by LEFM analyses based on strain, as described above. Crack propagation in vessel V-4 was considerably less extensive than that in vessel V-2 due to the higher test temperature of vessel V-4. A closeup view of the weld flaw in vessel V-4 is shown in Fig. 10.

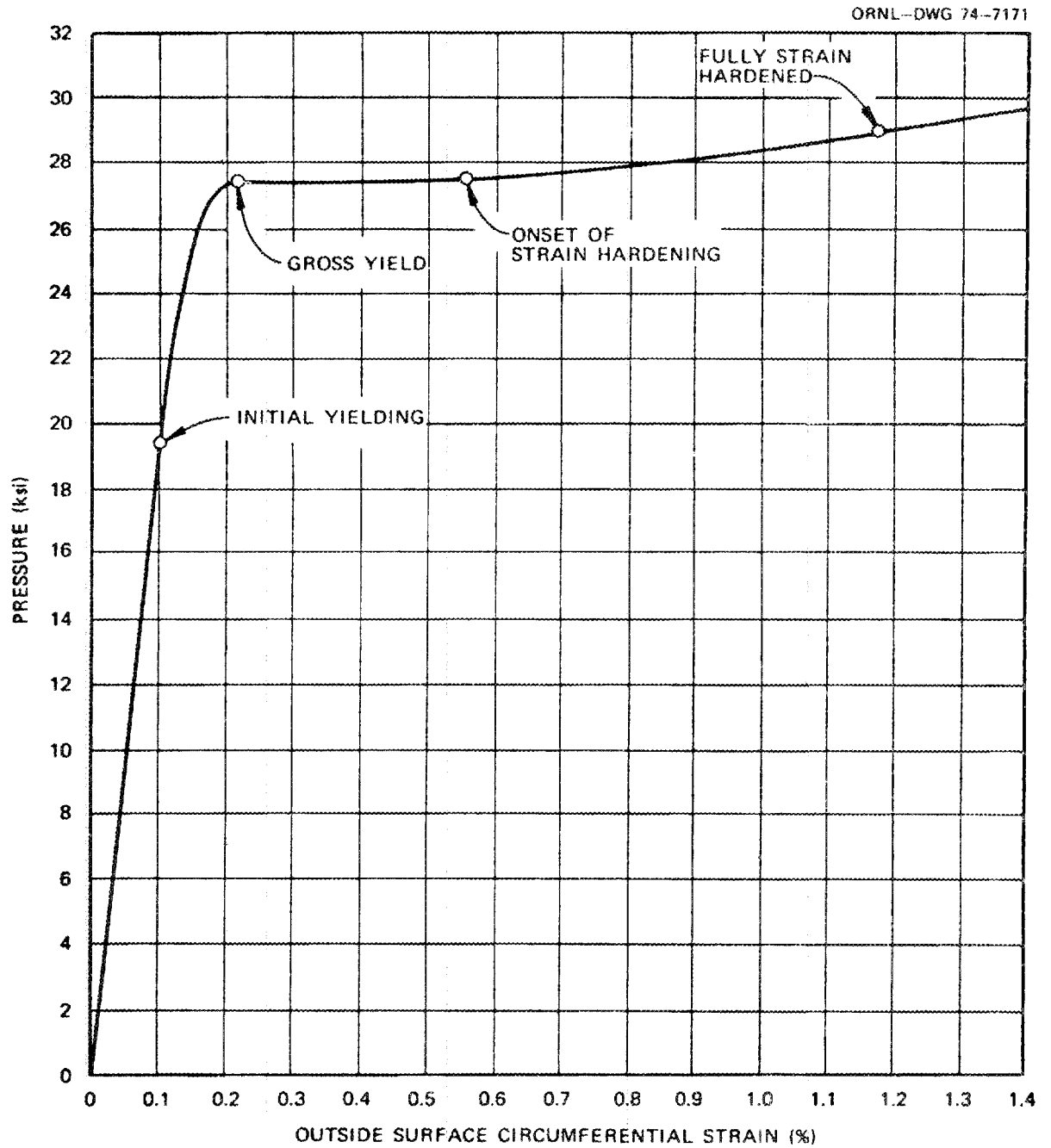


Fig. 8. Calculated pressure vs outside circumferential strain curve for intermediate test vessel.

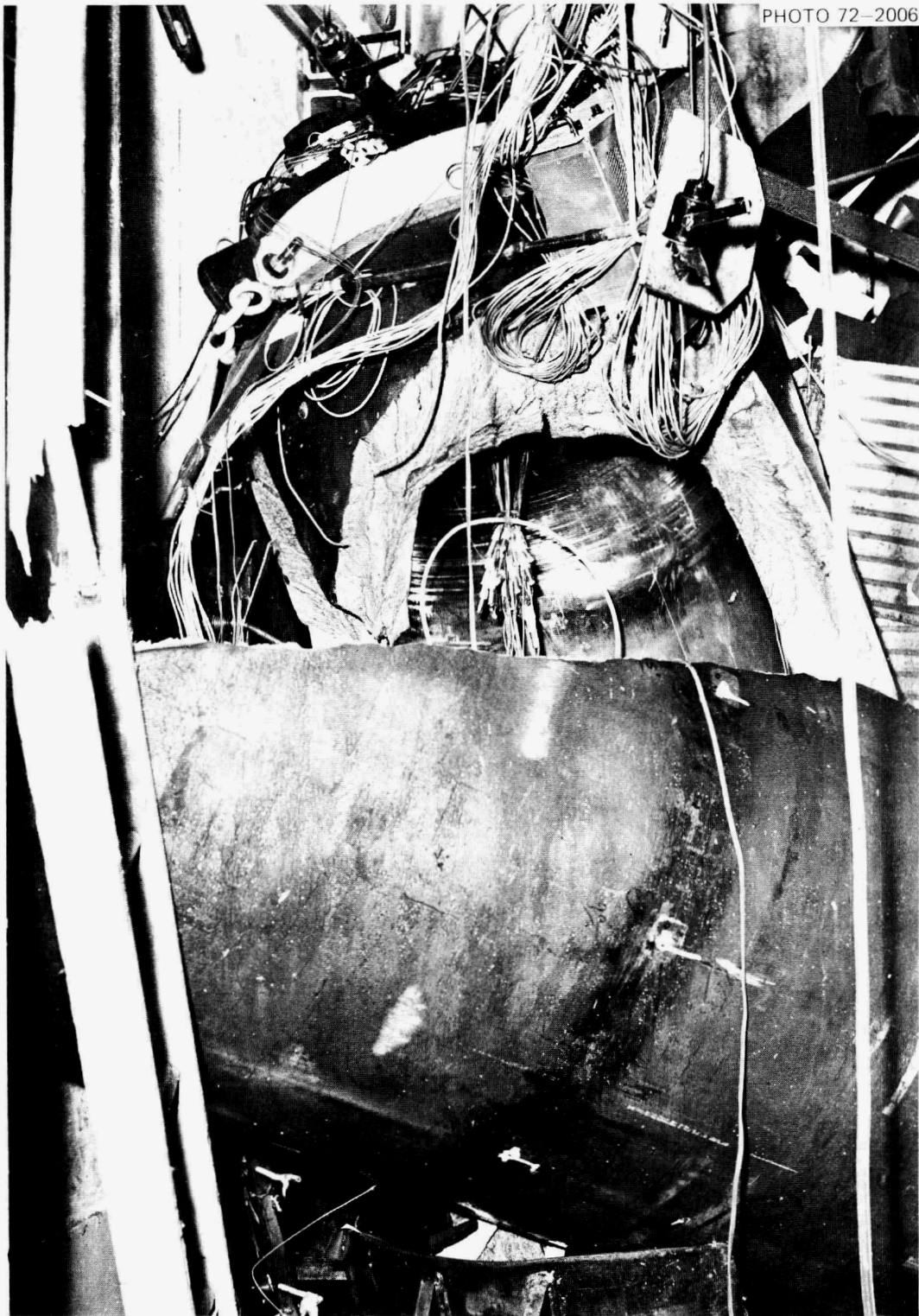


Fig. 9. Posttest view of intermediate test vessel V-2, tested at 32°F.



Fig. 10. Posttest view of outside surface weld flaw and fracture surface in intermediate test vessel V-4, tested at 75°F.

Vessel V-9, which had a flaw at the inside corner of a nozzle, was also tested at 75°F. The pressure and strain at failure for this vessel exceeded those calculated by an LEFM analysis based on strain, due to the fact that the inside nozzle corner is not a region of high transverse restraint even though it is a region of high stress concentration. The cylindrical region of this vessel yielded through the thickness before failure occurred at the flaw. Pretest crack arrest calculations for vessel V-9 indicated that crack arrest was unlikely, although possible. A fast fracture did occur, as expected, and crack arrest did not occur. A view of the failed nozzle region of vessel V-9 is shown in Fig. 11. Pieces of the test nozzle were separated from the vessel by the propagating fracture. Vessels V-2 and V-9 were the only vessels from which pieces were separated during fracture. Additional fracture analyses are being performed for vessel V-9.

Tests with Static Upper-Shelf Toughness

Vessels V-1 and V-3 were both tested at 130°F, which is the temperature above which plastic instability in the region of the flaw is expected to precede fracture even under plane strain conditions. Plastic instability occurs when the load-bearing area begins to contract at a rate greater than the rate at which the true stress on the same area increases due to the increase in strain; hence, plastic instability is a condition under which the capacity of a region to bear a load does not increase, and may decrease, with increasing strain. The only differences between vessels V-1 and V-3 were that the flaw in vessel V-3 was slightly smaller, and it was located in a longitudinal weld. The flaw in vessel V-1 was located in base metal. It can be seen from Table 3 that for both vessels V-1 and V-3, the failure pressure is very close to the calculated pressure for local plastic instability in the region of the flaw. This indicates that not only did the vessels have the capability of yielding through the thickness before failing but also the effect of the flaws in both vessels was mainly to reduce the load-bearing area of the vessel wall. At 130°F, the resistance of the vessel material to the continued propagation of a running



Fig. 11. Posttest view of fractured nozzle region in intermediate test vessel V-9, tested at 75°F.

crack is known to be less than its resistance to the onset of rapid fracture. Therefore, a rapidly propagating mixed mode fracture was expected and did occur in both vessels, as shown in Figs. 12 and 13. As indicated by Table 3, an LEFM analysis based on strain considerably underestimated the failure strains for both vessels. Several other methods of inelastic fracture analysis were also applied to vessel V-1, which was expected to (and did) fail in the plastic range after considerable stable crack growth. None of these methods overestimated the failure pressure by more than 10%.¹

Tests with Static and Dynamic Upper-Shelf Toughness

Vessel V-6 contained three part-through surface cracks and was tested at 190°F. Two of the flaws were outside surface flaws, one in base metal and the other in a longitudinal weld, and the third was an inside surface flaw in a longitudinal weld. Dynamic-tear test data indicated that at and above 190°F, fully plastic conditions would exist, and a crack arrest calculation indicated that a flat fracture would not propagate. Failure in V-6 initiated at the outside surface weld flaw after considerable stable crack growth. Full slant shear fracture extended from both ends of the flaw and arrested before reaching the ends of the vessel, as shown in Fig. 14. The measured values of pressure and strain at the onset of failure were nearly the same for vessels V-6 and V-3, because both vessels were tested in the temperature range in which the static initiation fracture toughness achieves its upper limiting value. However, the extent and mode of crack propagation were distinctly different for the two vessels, because at 130°F the crack propagation resistance of the test material is considerably less than its static initiation toughness, while at 190°F the former may even exceed the latter. The protection against fragment formation that is achieved by an increase in vessel operating temperature is dramatically illustrated by the comparison between the crack extension patterns that developed in vessel V-2 at 32°F (see Fig. 9) and in vessel V-6 at 190°F (see Fig. 14).

Vessel V-5, which was geometrically identical to vessel V-9, was tested at 190°F. Because, at this temperature, the propagation resistance of the nozzle material exceeded its static initiation toughness, the crack grew

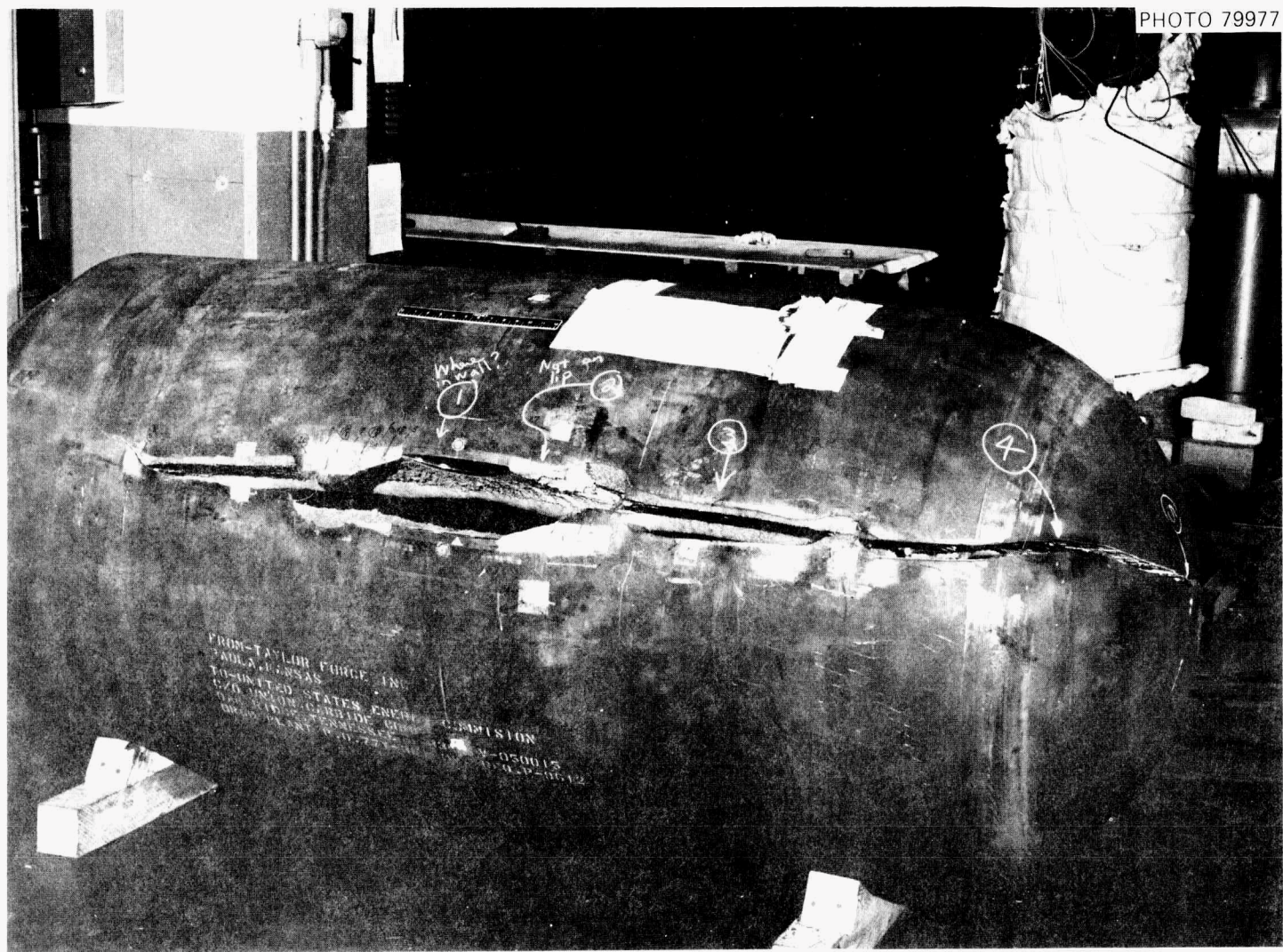


Fig. 12. Posttest view of intermediate test vessel V-1, tested at 130°F.

PHOTO 4055-73



Fig. 13. Posttest view of fracture in intermediate test vessel V-3, tested at 130°F.



Fig. 14. Posttest view of shear fracture in intermediate test vessel V-6, tested at 190°F.

stably under rising load until a small leak occurred at the outside nozzle corner closest to the closure end of the vessel, toward which the flaw was growing. A posttest view of vessel V-5 is shown in Fig. 15. The final failure pressures for vessels V-5 and V-9 were almost identical, although the outside circumferential strains on the vessel cylinders 180° from the nozzles were considerably different. This difference in strain occurred because both cylinders were almost exactly at the point of through-thickness yielding, at which considerable plastic strains occur with only a small change in load (see Fig. 8). Again the final failure pressure of vessel V-5 exceeded by a considerable margin the pressure estimated by an LEFM analysis based on strain, and the strains at failure at the opposite unflawed inside nozzle corner in both vessels V-5 and V-9 exceeded 6%. However, ultrasonic measurements of crack depth made from the outside nozzle corner indicated that stable crack growth had commenced at a pressure close to the LEFM estimated failure pressure.

Vessel V-7 was unique in the intermediate pressure vessel test series for several reasons. As shown by Fig. 16, it had by far the largest flaw (over 5 in. deep and 18 in. long); it was the only intermediate test vessel with a flaw that was sharpened by electron-beam welding and hydrogen charge cracking; and it was the only vessel with a surface flaw in the cylindrical region that leaked without fracturing. A view of vessel V-7 after testing is shown in Fig. 17. The flaw in vessel V-7 was carefully designed on the basis of failure data obtained from three 1/7-scale steel models containing long deep external surface flaws of different sizes. Analyses of these data revealed that if the fracture toughness of the thin ligament remaining between the crack tip and the inside surface of the vessel was considered to be a function of the ligament thickness, then an LEFM analysis agreed with the test data from all three models, despite the fact that the ligaments in each model were fully yielded before failure. The final dimensions of the flaw in vessel V-7 were calculated by the same method of analysis, which proved to be remarkably accurate with respect to the test data. The leak without fracture that occurred in vessel V-7 was predicted by a crack arrest analysis that recognized that the vessel wall thickness was insufficient to maintain full transverse restraint for an axially propagating crack. This leak occurred by the same process that had

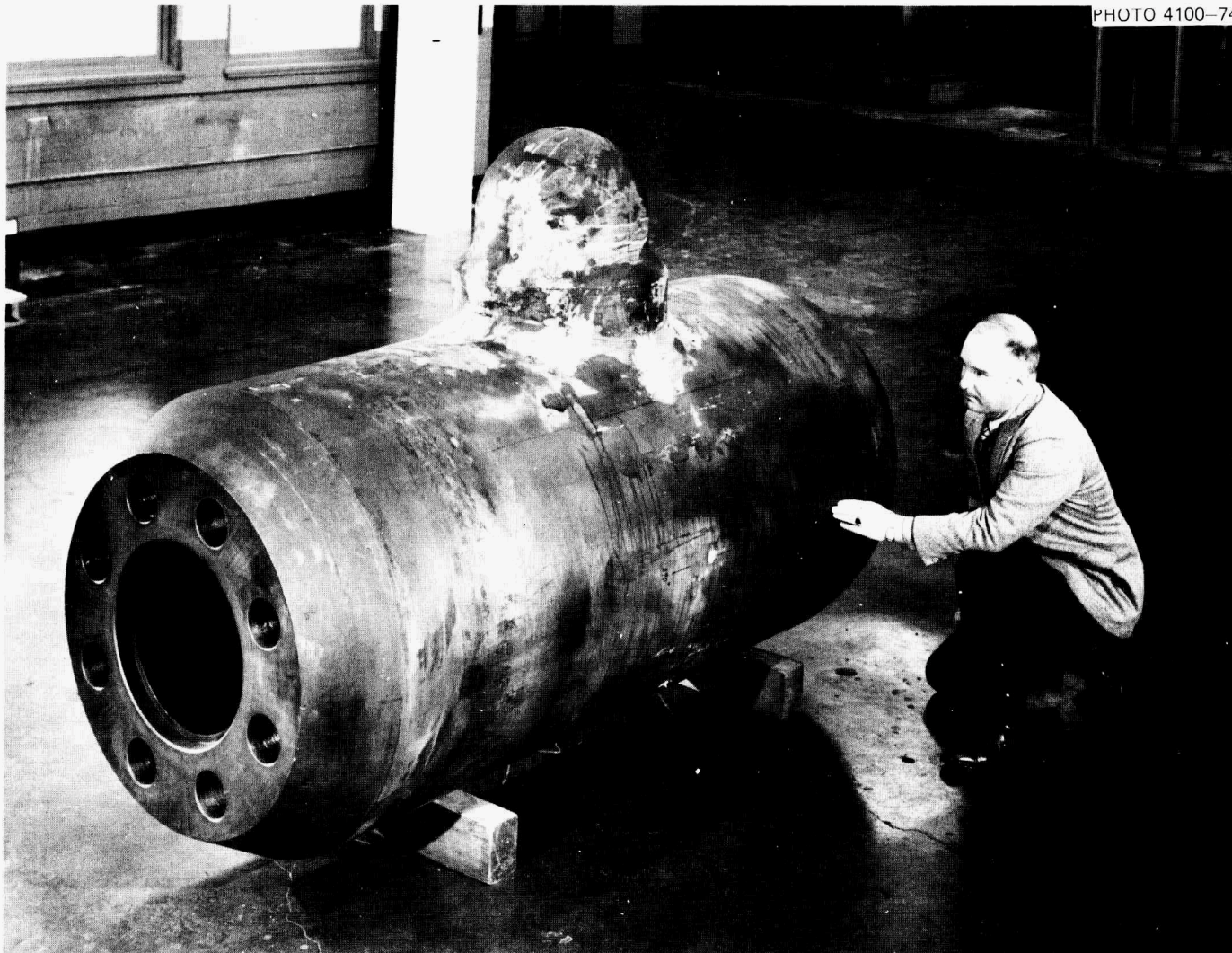


Fig. 15. Posttest view of intermediate test vessel V-5 that leaked without fracturing at 190°F.

ORNL-DWG 70-320R

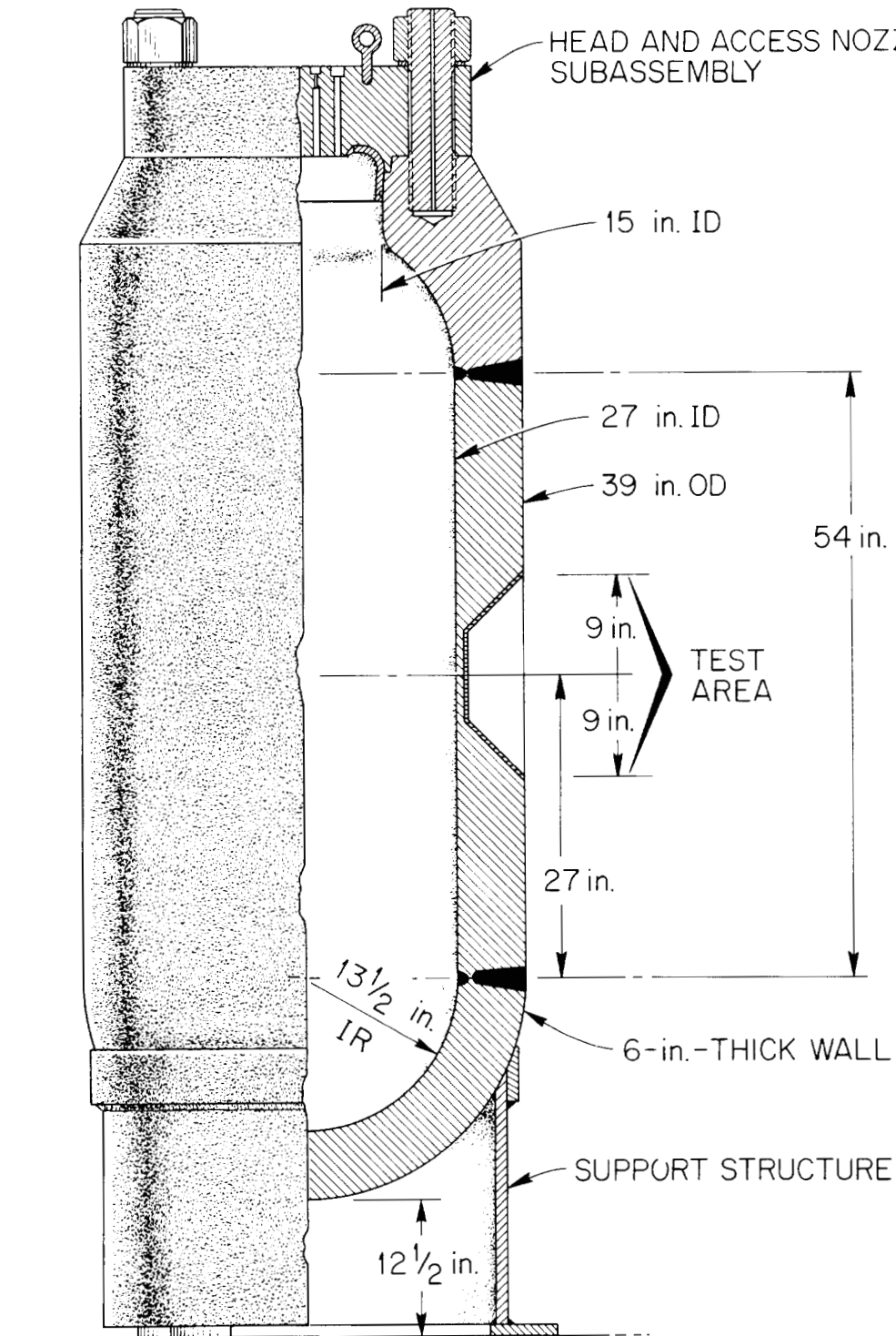


Fig. 16. Flaw design for intermediate test vessel V-7.

ORGDP
PHOTO 74-1810



Fig. 17. Posttest view of intermediate test vessel V-7 that leaked without fracturing at 126°F.

occurred in vessel V-5, namely, the stable growth of the crack through the remaining vessel wall, with no tendency for the crack to run fast. This mode of crack extension should be detectable by acoustic emission instrumentation and should therefore give warning of vessel unserviceability without immediate loss of function.

EXAMPLE CALCULATIONS FOR A HYPOTHETICAL REACTOR PRESSURE VESSEL

Definition of the Reference Computational Model

The relation between the intermediate test vessel experimental and analytical results just described and the safety against fracture of a full-scale reactor pressure vessel can be demonstrated with a calculational example. For this purpose, a reference calculational model representing a typical PWR vessel is defined by the information listed in Table 4. The fracture toughness at a given position in the vessel wall is determined by the neutron fluence, the copper content of the steel, the transition temperature shift corresponding to the aforementioned two parameters, and the chosen reference curve of fracture toughness vs temperature relative to the transition temperature. The relation between the neutron fluence and the radial distance from the inside surface of the vessel is based on Ref. 6, and is given in Table 4 as

$$F = 4 \times 10^{19} e^{-0.33x} , \quad (1)$$

where F is the neutron fluence (neutrons/cm², E ≥ 1 MeV) and x is radial distance from the inside surface (in.). The relation between the neutron fluence, the copper content, and the transition temperature shift is taken to be the set of curves developed by Litton,⁷ as shown in Fig. 18. For these calculations, a copper content of 0.20% was assumed, based on the data obtained for the A533, grade B, class 1 steel plates procured as test material by the HSST program.

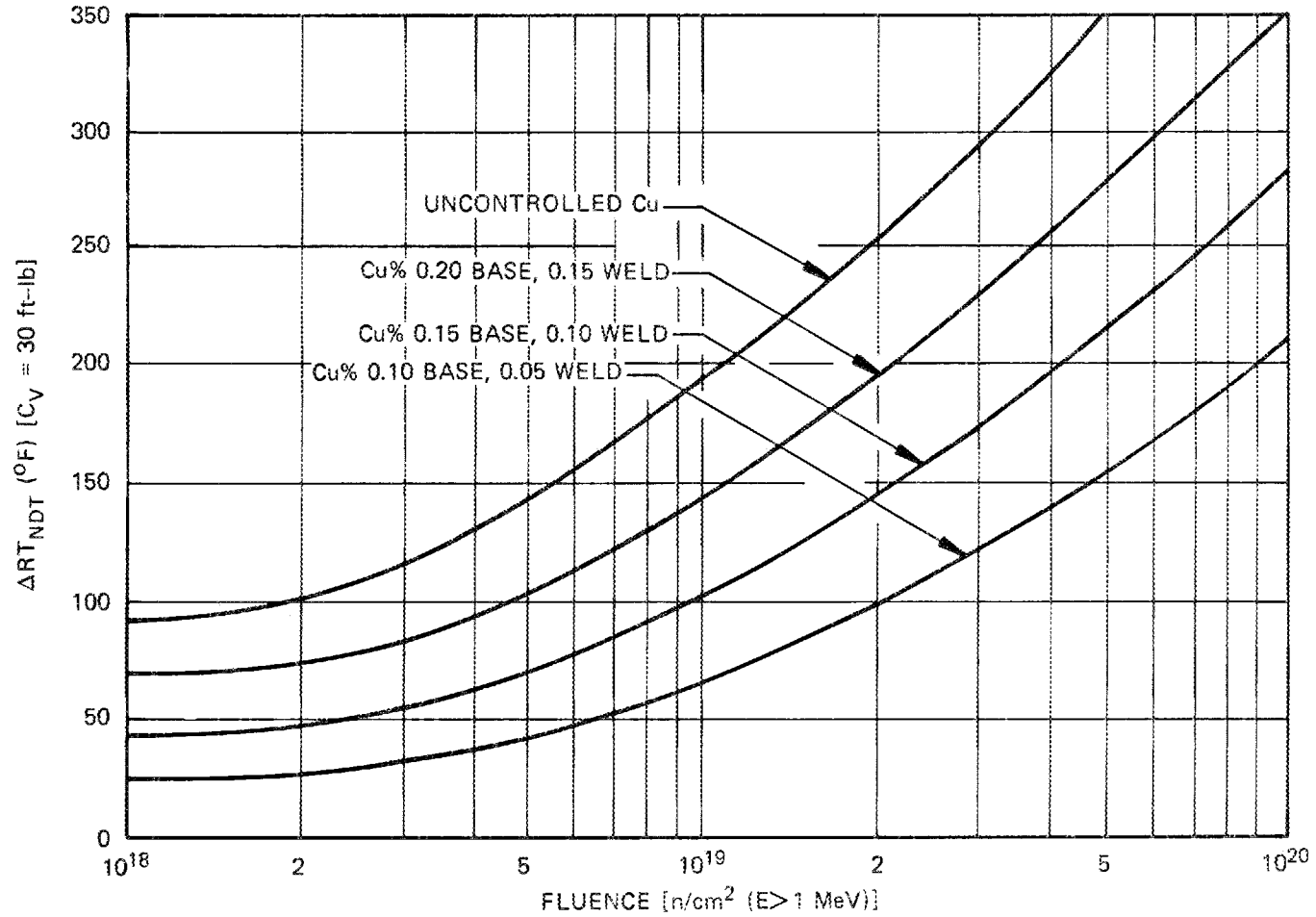


Fig. 18. Design curves for the maximum increase in reference transition temperature as a function of neutron fluence and copper content, for irradiation at 550°F (from Ref. 7).

Table 4. Specified conditions for reference
calculational model

| | |
|--|-------------------------------|
| Outside diameter, in. | 189 |
| Wall thickness, in. | 8.5 |
| Neutron fluence ($E \geq 1$ MeV), neutrons/cm ² | $4 \times 10^{19} e^{-0.33x}$ |
| Yield stress, ksi | 65 |
| Fracture toughness | |
| K_{Ic} source (unirradiated) | WCAP-7414 |
| RT_{NDT} (unirradiated), °F | +40 |
| ΔRT_{NDT} vs fluence and copper | |
| Source | Litton (October 1972) |
| % Copper | 0.20 |
| Flaw | |
| Shape | Semielliptical |
| a/2b | 0.36 |
| Location | Outside surface |
| Orientation | Axial |
| Depth, in. | 1/2, 1, 2, 3, 4 |
| Loading | Internal pressure |

Fracture Toughness Estimates

The reference curve of fracture toughness vs temperature for unirradiated material, which is to be shifted upward in temperature by the amount of the transition temperature shift determined from Fig. 18, was taken as the curve of valid static fracture toughness for A533, grade B, class 1 steel measured by Westinghouse.⁸ This curve can be fit, to a close

approximation, by the equation⁹

$$\frac{K_{IC}}{S_Y} = \frac{A_T}{T_\infty - T} \quad (2)$$

where K_{IC} is the plane strain fracture toughness (ksi $\sqrt{\text{in.}}$) and S_Y is the yield stress (ksi). The value of A_T given in Ref. 9 is 125 $\sqrt{\text{in.}}$ ($^{\circ}\text{F}$), and the value of T_∞ , based on the NDT temperature of 0°F given in Ref. 8, is given by

$$T_\infty = \text{NDT} + 125 \quad (3)$$

The value of A_T defines the shape of the K_{IC}/S_Y vs temperature curve and is assumed to be unaffected by irradiation.

Stress-Strain Properties and Pressure-Strain Calculations

The operating temperature true stress-strain diagram of the vessel steel assumed for this analysis is shown in Fig. 19. The variations in this diagram due to temperature and irradiation are neglected, which is a conservative assumption because irradiation and temperature decreases both cause the yield and ultimate stresses to increase, thereby raising the gross yield pressure of the vessel and the numerical value of K_{IC} if the ratio K_{IC}/S_Y is estimated independently as a function of temperature. The numerical parameters of the stress-strain diagram shown in Fig. 19 are listed in Table 5.

Using a closed-form elastic-plastic stress and strain analysis based on a trilinear approximation to the stress-strain diagram,⁵ the relation between internal pressure and outside circumferential strain is as shown in Fig. 20. The gross yield pressure (i.e., the pressure at which through-thickness yielding occurs in the reference calculational model) is 6126 psi. This pressure is just slightly less than three times the normal operating pressure of a PWR vessel, which is 2250 psi.

One difference between the pressure-strain diagram for the reference calculational model shown in Fig. 20 and the diagram for the intermediate test vessels shown in Fig. 8 is worth noting. The pressure difference

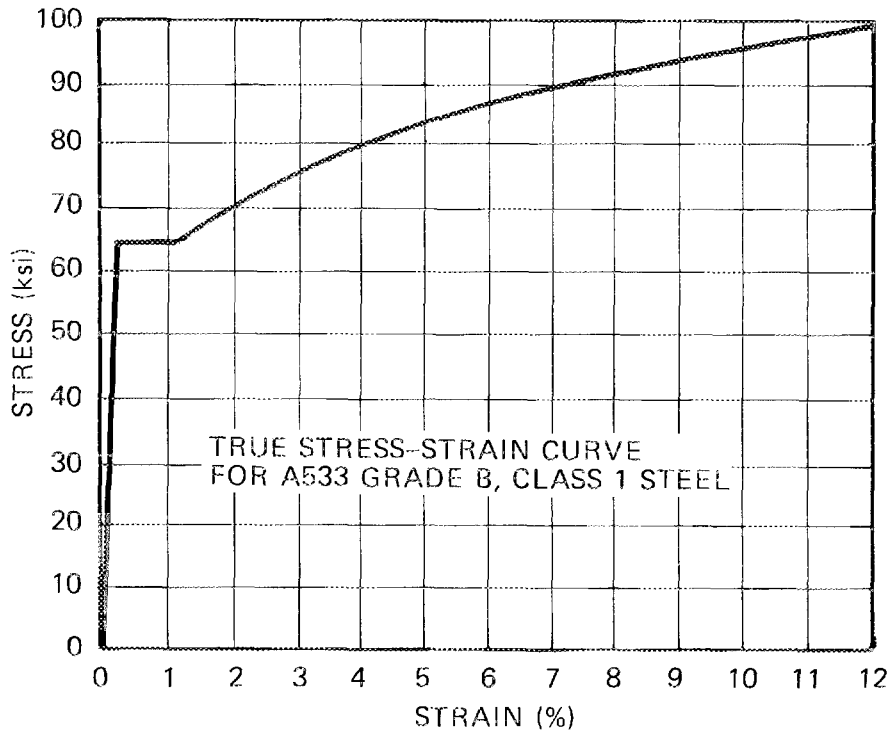


Fig. 19. True stress-strain diagram for A533 grade B class 1 steel assumed for analysis.

Table 5. Parameters of the stress-strain diagram used for analysis

| | |
|--|-----------------|
| Modulus of elasticity, ksi | 3×10^4 |
| Yield stress, ksi | 65 |
| Yield strain, % | 0.217 |
| Strain at the onset of strain hardening, % | 1.2 |
| Engineering ultimate stress, ksi | 87 |
| Necking strain, % | 12.0 |
| True ultimate stress, ksi | 98.1 |

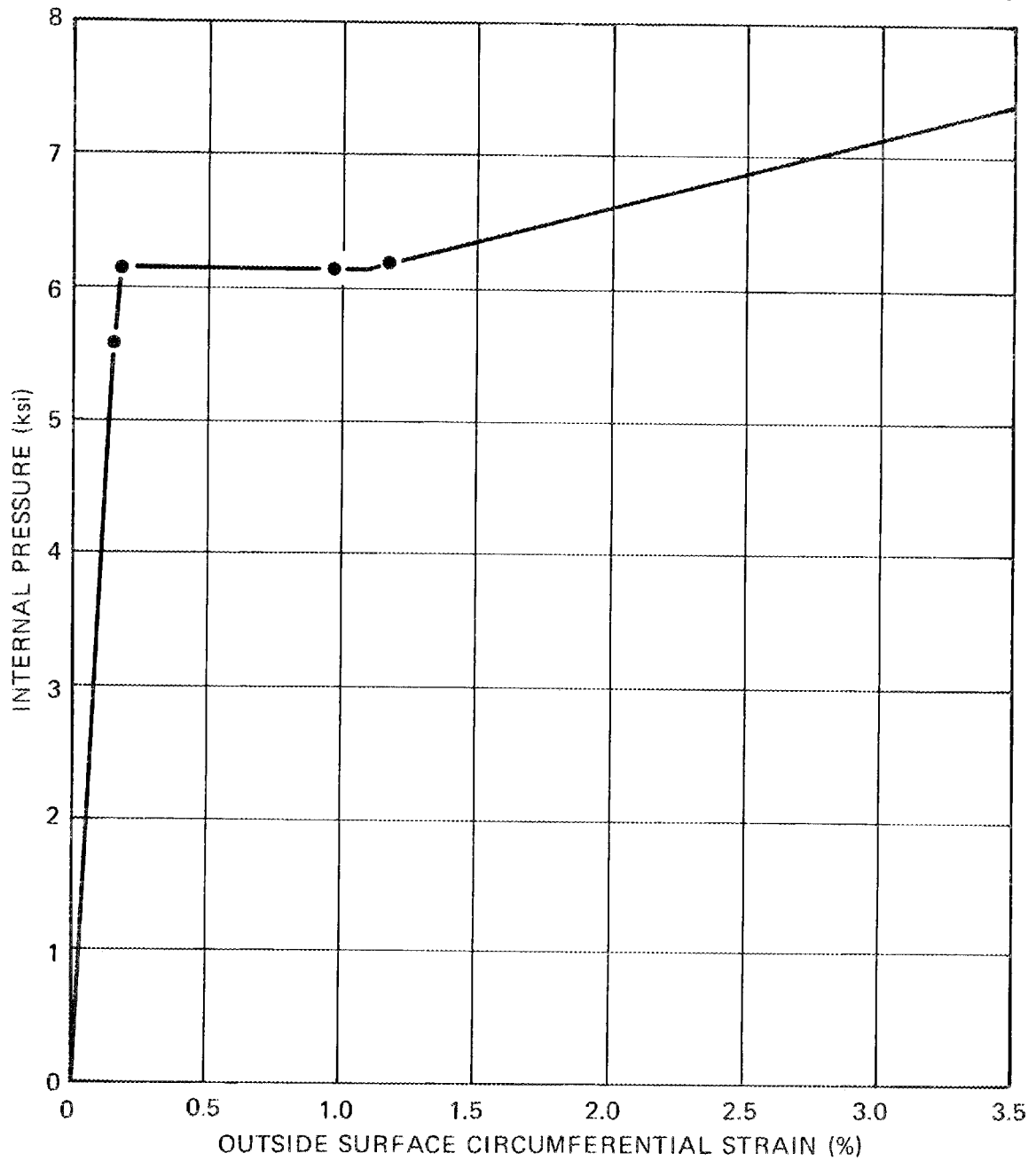


Fig. 20. Calculated pressure vs outside circumferential strain curve for the reference calculational model.

between initial and complete yielding is proportionally less for the reference calculational model than for the intermediate test vessels, because of the smaller thickness to diameter ratio of the former. This means that in the cylindrical region, elastic-plastic fracture analysis methods are not as necessary below the gross yield pressure for the reference calculational model as for the intermediate test vessels. However, for regions of stress concentration such as nozzle corners, where yielding occurs sooner and progresses more gradually, elastic-plastic fracture analysis methods should again be of considerable importance prior to gross yielding. As will be shown, elastic-plastic fracture analysis methods are definitely required to obtain realistic results above the gross yield pressure.

Code Design Pressure

Based on Section III of the ASME code, the code design pressure for the reference calculational model is given by

$$p_{all} = \frac{S_m}{\frac{1}{(Y-1)} + \frac{1}{2}}, \quad (4)$$

where p_{all} is the allowable pressure, S_m is the allowable stress intensity, and Y is the ratio of the outer to the inner radii of the vessel. Using the value of $S_m = 26.7$ ksi given by Section III of the ASME code, the code design pressure for the reference calculational model is 2515 psi, which is about 10% greater than the normal operating pressure of 2250 psi.

Upper-Shelf Plastic Instability Pressures

An upper limit to the failure pressure of a cylindrical pressure vessel containing an external part-through surface crack can be estimated as the pressure at which plastic instability occurs in the region surrounding the flaw. This pressure can be estimated from the equation¹

$$p_f = S_0^* (Y-1) \left(1 - \frac{A_c}{A} \right), \quad (5)$$

where S_0^* is a plastic instability flow stress estimated as about 1.07 times the average of the yield and ultimate stresses, A_c is the crack area, and A is the effective load-bearing area containing the flaw. The areas A_c and A are calculated from

$$A_c = \frac{\pi(a + \Delta a)(b + \Delta b)}{2} , \quad (6)$$

and

$$A = [2(b + \Delta b) + w]w , \quad (7)$$

where Δa and Δb are estimates of the stable crack growth that occurs prior to maximum load. Using a value of $S_0^* = 81.3$ ksi and allowing for 20% stable crack growth prior to maximum load, a value selected to be slightly more conservative than the value of 15% used in the calculations for vessels V-1, V-3, and V-6 summarized in Table 3, results in the plastic instability pressures and strains as functions of initial flaw size listed in Table 6. For the pressures in the strain-hardening range of the pressure-strain curve shown in Fig. 20, the failure strains listed in

Table 6. Plastic instability pressures and strains for the reference calculational model

| Initial flaw size (in.) | Pressure (psi) | Strain (%) . |
|-------------------------------|-------------------|-----------------|
| 0.5 | 7960 | 4.60 |
| 1.0 | 7790 | 4.27 |
| 2.0 | 7250 | 3.23 |
| 3.0 | 6590 | 1.96 |
| 4.0 | 5860 | 0.17 |

Table 6 are calculated from

$$\lambda = \frac{p - 5.57}{0.520} , \quad (8)$$

where p is in ksi and λ is in percent.

Linear Elastic Fracture Mechanics Calculations

Estimates of fracture pressure vs temperature were made by LEFM for the flaw sizes listed in Table 6 for fracture pressures equal to or less than the gross yield pressure. Between the initial and the gross yield pressures, the failure strains were calculated directly by LEFM, as previously described, and the failure pressures were then calculated from the pressure-strain curve given in Fig. 20. These calculations were originally extended to the plastic instability strains, but the results showed that the fracture toughness values required to reach plastic instability failure strains were unrealistically high, because of the extreme conservatism of LEFM based on strain in the cylindrical region, above the gross yield pressure. It was thus determined that a more realistic type of elastic-plastic fracture analysis would be necessary above the gross yield pressure in order to prove that upper-shelf plastic instability conditions can be reached with physically reasonable levels of fracture toughness. The elastic-plastic analysis will be discussed after the major details of the LEFM analysis have been explained.

Following Ref. 10, the linear elastic stress intensity factor at the deepest point of each flaw was calculated from

$$K_I = C S_s \sqrt{\pi a} , \quad (9)$$

where C is a nondimensional shape factor, S_s is the outside surface circumferential stress, and a is the flaw depth. The shape factor is estimated from

$$C = \frac{M_1 M_2}{\Phi} , \quad (10)$$

where M_1 is the front-face free-surface magnification factor which, for the computed elastic stress distribution in the reference calculational

model, is given by¹⁰

$$M_1 = 1.025 + 0.055 \left(\frac{a}{w} \right) ; \quad (11)$$

M_2 is the back-face free-surface magnification factor given by

$$M_2 = \left(\frac{\tan \frac{\pi a}{2w}}{\frac{\pi a}{2w}} \right)^{1/2} ; \quad (12)$$

and Φ is the complete elliptic integral of the second kind which is closely approximated by the expression

$$\Phi^2 = 1 + 4.593 \left(\frac{a}{2b} \right)^{1.65} . \quad (13)$$

The resulting elastically computed shape factors are listed in Table 7.

Table 7. Calculated LEFM shape factors
for external part-through surface
cracks in the reference
calculational model

| Flaw depth a (in.) | Shape factor C |
|-----------------------|----------------|
| 0.5 | 0.757 |
| 1.0 | 0.762 |
| 2.0 | 0.781 |
| 3.0 | 0.812 |
| 4.0 | 0.858 |

By elastic stress analysis, the relations between the internal pressure and the outside surface circumferential stress and strain for the reference calculational model are

$$s_s = 9.641p , \quad (14)$$

and

$$\lambda = \frac{P}{36.61} \quad , \quad (15)$$

respectively, where S_s and p are in ksi and λ is in percent.

The resulting values of fracture pressure vs flaw size and temperature, calculated by LEFM for pressures equal to or less than the gross yield pressure, are plotted in Fig. 21, along with the elastic-plastic fracture analysis results for pressures exceeding the gross yield pressure and a Section III, Appendix G analysis, both of which will be discussed below.

Elastic-Plastic Fracture Mechanics Calculations

The elastic-plastic fracture analysis results plotted in Fig. 21 for pressures exceeding the gross yield pressure of 6126 psi were obtained by the tangent modulus method of analysis, which is described in detail in Appendix H of Ref. 5. The basic equation of the tangent modulus method is^{1,5}

$$d\epsilon \sqrt{\rho} = 2C \sqrt{a} \sqrt{\frac{E_g}{E_s}} d\lambda \quad , \quad (16)$$

where ϵ and ρ are the notch root strain and root radius, respectively, C is the LEFM shape factor, a is the crack depth, E_g is the tangent modulus corresponding to the gross strain, E_s is the strain-hardening tangent modulus at the notch tip, and λ is the nominal (gross) strain at the flaw location. The value of the quantity $\epsilon\sqrt{\rho}$ at fracture is obtained by integrating the right side of Eq. (16) and is directly related to the value of K_{Ic} . Because the tangent modulus method of analysis is an incremental rather than a total strain method of elastic-plastic fracture analysis, it is ideally suited to determining the increases in fracture toughness required to extend the fracture strength of the reference calculational model from the gross yield pressure to the plastic instability pressures for the specified flaw sizes. For this analysis, a part-through surface

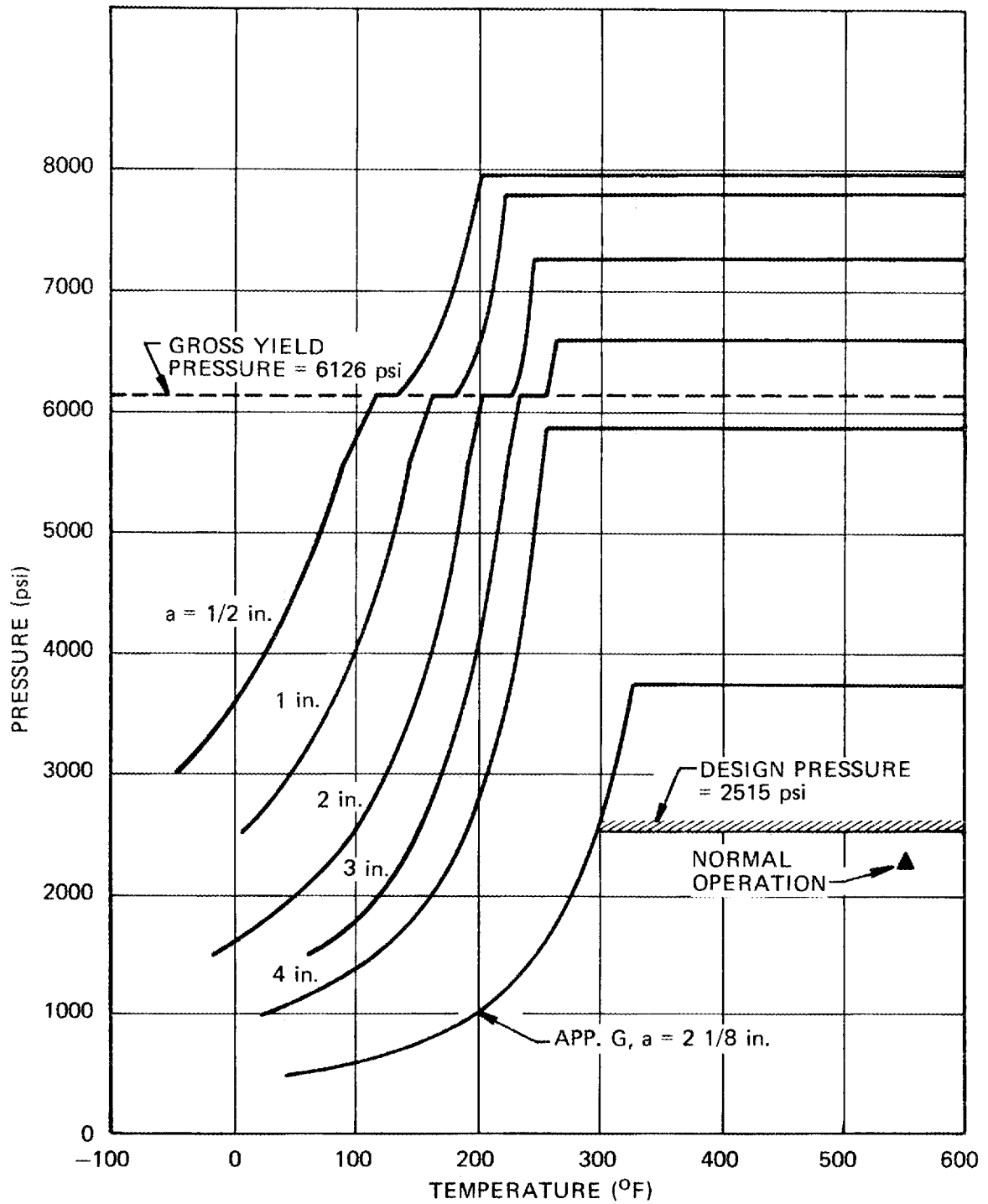


Fig. 21. Calculated fracture analysis diagram for external surface flaws in the reference calculational model.

cracked tensile specimen model was used, assuming full transverse restraint and an effective width/thickness ratio of 5. The strain-hardening tangent modulus was estimated from Fig. 19 as $3.06 \text{ ksi} \cdot (\%)^{-1}$. The fracture toughness values required for the reference calculational model to reach its plastic instability strength for each flaw size are listed in Table 8. By comparison with Table 2, it can be seen that these toughness values are physically reasonable. The required fracture toughness value for the 4-in.-deep flaw is less than the required values for the 1-, 2-, and 3-in.-deep flaws because local plastic instability around the 4-in.-deep flaw occurs prior to the onset of gross yielding.

Table 8. Fracture toughness values required for the reference calculational model to reach plastic instability conditions

| Flaw depth a (in.) | Fracture toughness K_{Ic} (ksi $\sqrt{\text{in.}}$) |
|-------------------------|---|
| 0.5 | 173 |
| 1.0 | 249 |
| 2.0 | 341 |
| 3.0 | 381 |
| 4.0 | 183 |

ASME Code, Section III, Appendix G Calculations

For comparative purposes, a calculation was made by the method prescribed by Appendix G of Section III of the ASME Boiler and Pressure Vessel Code (see the 1974 edition of Division 1, subsection NA, pp. 489-495). This analysis is based on a lower bound to the crack arrest toughness, rather than on the static fracture toughness curve, and also incorporates a factor of safety of 2.0 on pressure-induced stresses. The fracture toughness curve is represented by the equation¹¹

$$K_{IR} = 26.777 + 1.223 \exp [0.014493 (T - RT_{NDT}) + 160] \quad (17)$$

For this analysis, the upper limit of the K_{IR} curve was assumed to be 200 ksi $\sqrt{\text{in}}$. Appendix G specifies a reference flaw depth that is one-quarter of the vessel wall thickness. For the reference calculational model, the reference flaw depth is therefore 2 1/8 in. As shown in Fig. 21, the curve resulting from the Appendix G analysis lies well below the other calculated curves, but still lies above both the design pressure and the operating pressure at the operating temperature.

Figure 21 implies that the margins of safety between failure pressure and design pressure that were observed for the intermediate test vessels are also representative of the margins of safety that exist for full-scale vessels, considering external surface flaws of the same size located in sound material. The conservatism of the ASME code is also illustrated by the example calculations.

DISCUSSION

The intermediate pressure vessel tests can be distinguished from many other structural component fracture tests by the fact that they were done with adequately sharpened flaws, with prior measurements of fracture toughness, prior elastic and plastic scale model tests, and accurate measurements of load, strain, and surface crack opening displacement up to failure. The results obtained indicate that the material tested has a high resistance to fracture even in the presence of large and sharp flaws. With respect to fracture analysis methods, linear elastic fracture mechanics, expressed in terms of strain, has been accurate under plane strain conditions up to the onset of gross yielding, and other methods of analysis have been applied successfully in the plastic range. Methods for calculating fracture toughness from small specimens that fail in the plastic range have been developed and successfully applied to the fracture analyses of the intermediate test vessels.

The fracture strengths achieved by the intermediate test vessels can be judged overall by several different standards, all of which have validity. The first standard is the comparison between the pressure that would be allowed in the vessel, according to the ASME code, and the measured failure pressure. As seen in Table 3, the ratio of the failure pressure

p_f to the design pressure p_d is between 2.7 and 3.3 for all the vessels except for vessel V-7, which contained a very long flaw extending almost completely through the vessel wall. In addition, vessel V-7 leaked instead of fracturing, as did vessel V-5, which contained a flaw in the stress concentration region of the inside nozzle corner.

A second basis for judging the flaw tolerating ability of the vessels is their ability to yield through the thickness before failing. The specified stress limits for nuclear pressure vessels under full-load operating conditions are based on the assumption that all parts of a vessel can reach a condition of yielding through the thickness, including the development of substantial plastic strains, with no ill effects to the vessel even in the presence of sharp flaws. In other words, it is implicitly assumed that under operating conditions the vessel cannot fail by fast fracture in the elastic range of stress. The intermediate pressure vessel test data obtained thus far substantiate this assumption, provided that material properties remain adequate and a flaw does not exist that is large compared to the thickness of the vessel wall, which is unlikely. In other words, small undetected flaws are not expected to constitute a safety hazard under operating conditions. Therefore, only inadequate material properties, large flaws, or extreme loading conditions exceeding the values permitted by present codes remain as possible causes of vessel malperformance under operating conditions. The intermediate test vessel experimental and analytical data thus provide confirmation of the existence of the intended margin of safety for full-scale vessels.

REFERENCES

1. R. W. Derby et al., *Test of 6-Inch-Thick Pressure Vessels, Series 1. Intermediate Test Vessels V-1 and V-2*, ORNL-4895 (February 1974).
2. F. J. Witt and T. R. Mager, *A Procedure for Determining Bounding Values on Fracture Toughness K_{Ic} at Any Temperature*, ORNL-TM-3894 (October 1972).
3. J. G. Merkle, R. G. Berggren, and W. J. Stelzman, "Compliance and Fracture Toughness Calculations for Notched Bend Specimens," *Quarterly Progress Report on Reactor Safety Programs Sponsored by the NRC Division of Reactor Safety Research for October-December 1974*, ORNL-TM-4805, Vol. II, pp. 4-10.

4. J. G. Merkle and H. T. Corten, "A J Integral Analysis for the Compact Specimen, Considering Axial Force as Well as Bending Effects," *Journal of Pressure Vessel Technology, ASME*, Vol. 96, Series J, No. 4, pp. 286-92 (November 1974).
5. R. H. Bryan et al., *Test of 6-Inch-Thick Pressure Vessels, Series 2. Intermediate Test Vessels V-3, V-4, and V-6*, ORNL-5059 (to be published).
6. R. D. Cheverton, "Thermal Shock Investigations," *Quarterly Progress Report on Reactor Safety Programs Sponsored by the NRC Division of Reactor Safety Research for October-December 1974*, ORNL-TM-4805, Vol. II, pp. 71-98.
7. F. B. Litton, *The Effect of Residual Elements on the Sensitivity of Pressure Vessel Steels to Irradiation Embrittlement*, draft memorandum, Materials Engineering Branch, Directorate of Licensing, October 1973.
8. W. O. Shabbits, W. H. Pryle, and E. T. Wessel, *Heavy Section Fracture Toughness Properties of A533 Grade B, Class 1 Steel Plate and Submerged-Arc Weldment*, WCAP-7414 (also HSSTP-TR-6) (December 1969).
9. J. G. Merkle, "Fracture Safety Analysis Concepts for Nuclear Pressure Vessels, Considering the Effects of Irradiation," *Journal of Basic Engineering, ASME*, Vol. 93, Series D, No. 2, pp. 265-73 (June 1971).
10. J. G. Merkle, "Stress Intensity Factor Estimates for Part-Through Surface Cracks in Plates Under Combined Tension and Bending," *Quarterly Progress Report on Reactor Safety Programs Sponsored by the Division of Reactor Safety Research for July-September 1974*, ORNL-TM-4729, Vol. II, pp. 3-32.
11. PVRC Ad Hoc Group on Toughness Requirements, "PVRC Recommendations on Toughness Requirements for Ferritic Materials," *WRC Bulletin 175*, Welding Research Council, August 1972.

Internal Distribution

- | | |
|-------------------------|--|
| 1. M. Bender | 27-36. J. G. Merkle |
| 2. R. G. Berggren | 37. S. E. Moore |
| 3. R. H. Bryan | 38. F. H. Neill |
| 4. J. Buchanan | 39. H. A. Pohto (Y-12) |
| 5. J. P. Callahan | 40. H. Postma |
| 6. D. A. Canonico | 41. M. N. Raftenberg |
| 7. R. D. Cheverton | 42. G. C. Robinson |
| 8. C. E. Childress | 43. C. D. St. Onge (Y-12) |
| 9. J. M. Corum | 44-45. Myrtle Sheldon |
| 10. W. B. Cottrell | 46. C. B. Smith |
| 11. G. G. Fee | 47. G. C. Smith |
| 12. M. H. Fontana | 48. J. E. Smith |
| 13. W. R. Gall | 49. I. Spiewak |
| 14. M. J. Goglia | 50. W. J. Stelzman |
| 15. W. L. Greenstreet | 51. J. J. Taylor |
| 16. R. C. Gwaltney | 52. D. G. Thomas |
| 17. M. R. Hill | 53. D. B. Trauger |
| 18. P. P. Holz | 54. J. R. Weir, Jr. |
| 19. H. W. Hoffman | 55-152. G. D. Whitman |
| 20. K. K. Klindt | 153. W. J. Wilcox |
| 21. R. N. Lyon | 154. Patent Office |
| 22. R. E. MacPherson | 155-156. Central Research Library |
| 23. W. R. Martin | 157. Y-12 Document Reference Section |
| 24. W. J. McCarthy, Jr. | 158-162. Laboratory Records Department |
| 25. R. W. McClung | 163. Laboratory Records, RC |
| 26. J. R. McGuffey | |

External Distribution

- 164-171. Director, Office of Nuclear Regulatory Research, Nuclear Regulatory Commission, Washington, D.C. 20555
172. Director, Reactor Division, Energy Research and Development Administration, Oak Ridge Operations Office
173. Director, Research and Technical Support Division, Energy Research and Development Administration, Oak Ridge Operations Office
- 174-310. Special HSST Distribution
- 311-570. Given distribution under categories NRC-1, NRC-5